Fall 2015

Evaluation of particle penetration and breathing resistance of N95 filtering face-piece respirators and uncertified dust masks

Joel Amilcar Ramirez
University of Iowa

EVALUATION OF PARTICLE PENETRATION AND BREATHING RESISTANCE OF N95 FILTERING FACE-PIECE RESPIRATORS AND UNCERTIFIED DUST MASKS

by

Joel Amilcar Ramirez

A thesis submitted in partial fulfillment
of the requirements for the Doctor of Philosophy degree in
Occupational and Environmental Health (Industrial Hygiene)
in the Graduate College of
The University of Iowa

December 2015

Thesis Supervisor: Professor Patrick O'Shaughnessy

Graduate College
The University of Iowa
Iowa City, Iowa

CERTIFICATE OF APPROVAL

_____

PH.D. THESIS

_____

This is to certify that the Ph.D. thesis of

Joel Amilcar Ramirez

has been approved by the Examining Committee for the thesis requirement for the Doctor of Philosophy degree in Occupational and Environmental Health (Industrial Hygiene) at the December 2015 graduation.

Thesis Committee: _____
Patrick O'Shaughnessy, Thesis Supervisor

_____
Thomas M. Peters

_____
T. Renee Anthony

_____
Matthew W. Nonnenmann

_____
Nathan B. Fethke

To family and friends, thank you for your support

ACKNOWLEDGMENTS

I would like to offer my thanks to my advisor, Patrick, for his guidance and advice. I want to thank my committee members for their time and expertise. I am very grateful to the students for their support during this endeavor. This study would not have been possible without the research training and financial support from the Heartland Environmental Research Center, funded by the National Institute for Occupational Safety and Health. Finally, thanks to faculty and staff that helped me throughout the projects and education.

ABSTRACT

The research presented in this doctoral dissertation strived to increase knowledge with respect to respirators performance in the workplace by evaluating particle penetration and breathing resistance (BR) of N95 filtering face-piece respirators (FFRs) under simulated air environmental conditions, determining maximum particle penetration of uncertified dust masks (UDMs) against sodium chloride (NaCl) and BR of UDMs and FFRs when challenged against Arizona road dust (ARD), and evaluating BR of FFRs while performing power washing in swine rooms.

A novel test system was used to measure particle penetration and BR of two N95 FFRs under modified environmental conditions. NaCl particle penetration through the FFR was measured before and after the BR test using a scanning mobility particle sizer. BR of the FFR was measured by mimicking inhalation and exhalation breathing, while relative humidity and temperature were modified. BR was evaluated for 120 min under cyclic flow and four temperature and relative humidity air conditions. The BR of the FFRs was found to increase significantly with increasing relative humidity and lowering temperature upstream the FFR ($p < 0.001$). Measured particle penetration was not influenced by the simulated air environmental conditions. Differences in BR was observed between FFRs indicating that FFRs filtering media may perform differently under high relative humidity in air.

In the second study, the maximum particle penetration of five commercially available UDMs was evaluated against NaCl aerosol. Particle penetration was carried out as specified by National Institute for Occupational Safety and Health (NIOSH) to certify N95 FFRs (42 CFR Part 84). Particle penetration was found to vary between 3% and 75%

at the most penetrating particle size. In addition, the effect of mass loading on BR of UDMs and FFRs over time was evaluated. ARD was used as the loading dust and BR was measured for 120 min on UDMs and FFRs. BR was found to increase differently between the tested UDMs and FFRs. Further analysis of the UDMs and FFRs external layer suggest that the development of the particle dust cake during mass loading may be influenced by differences of the external layer.

In the third study, field research was conducted to evaluate BR of two N95 FFRs while performing power washing in swine rooms. A member of the research team wore the FFR while power washing swine rooms. Every 30 min the team member stopped power washing, BR was measured and power washing continued. At the end of the 120 min trial, the FFR model was switched and the team member continued to power wash the rest of the room. Results demonstrated that BR of the tested FFRs did not increased during power washing in swine rooms (FFR 1, $p = 0.40$; FFR 2, $p = 0.86$). Power washing was found to have an effect in the temperature and relative humidity inside the rooms. Based on this study, FFR wearer should expect no increase in BR over 8 hr of power washing, decrease health risk by wearing the FFR and no need to replace the FFR during the power washing task.

PUBLIC ABSTRACT

This study evaluated two properties of commercially available respirators and dust masks: particle penetration and breathing resistance. Particle penetration describe the fraction of particle passing through the respirator and dust mask. Breathing resistance describe how difficult is to breathe through when using the respirator or dust mask.

An equipment setup was constructed to measure the particle penetration and breathing resistance of respirators and dust masks. Particle penetration of respirators and dust masks was evaluated against sodium chloride aerosol. Breathing resistance of two respirators was evaluated in simulated air temperature and relative humidity conditions. Also, Arizona road dust was used to evaluate the breathing resistance of respirators and dust masks. Finally, breathing resistance of two respirators was evaluated while power washing swine rooms.

Breathing resistance of respirators increased with increasing relative humidity and low temperature outside the respirators. Particle penetration did not changed under simulated temperature and relative humidity conditions. Particle penetration through dust masks varied greatly against sodium chloride aerosol. Arizona road dust affected the breathing resistance differently of all the tested respirators and dust masks. The breathing resistance of two respirators was unaffected during the power washing task in swine rooms.

Overall differences were observed in particle penetration and breathing resistance in the tested respirators and dust masks. However, further research is needed with additional respirators and dust masks to observe if differences are encounter in multiples respirator and dust mask models.

TABLE OF CONTENTS

LIST OF TABLES

LIST OF FIGURES

CHAPTER I

INTRODUCTION

Filtering Facepiece Respirators and dust masks are air filters composed of a mesh of fibers with a distinct fiber diameter and material that removes contaminants from the air (NIOSH, 1995). Filtering face-piece respirators (FFRs) are well-recognized personal protective equipment (PPE) used by workers to provide protection against airborne particulate in a variety of occupational settings (NIOSH, 1995). An estimated five million workers are required to wear respirators daily throughout the United States (OSHA, 2009). Agriculture, manufacturing, construction, and mines are some of the industries that are concerned about the use of FFRs (OSHA, 1999). FFRs worn correctly will protect the wearer, and can prevent acute or chronic health symptoms to the wearer.

Breathing resistance (BR) and efficiency of particle removal are the principal criteria for measuring FFR performance (Friedlander, 1958). The National Personal Protective Technology Laboratory (NPPTL) test FFRs using the method described in the Code of Federal Regulation (42 CFR 84.180 – 84.181) (NIOSH, 1995). The NPPTL tests FFRs in a laboratory setting where the temperature (77°F) and relative humidity (30%) are controlled. However, environmental conditions where FFRs are used differ from a controlled laboratory setting. For example, power washing is a task that generates high humidity conditions and is performed in varying temperatures.

Swine farm workers experience occupational exposure to airborne dusts when performing power washing (Larsson et al. 2002). Power washing operations performed in swine farms are associated with the generation of dust particles that accumulate in the upper respiratory tract (Larsson et al. 2002). Dust particles inside these buildings comes from a variety of sources,

including feed particles, skin dander, dried fecal material, and other sources (Donham et al. 1986). Previous studies have demonstrated the adverse respiratory effects of workers exposed to dust in indoor swine buildings (Zejda et al. 1993; Larsson et al. 1997; Wang et al. 1997; Dosman et al. 2000; Larsson et al. 2002; Sowiak et al. 2012). In one study, personal dust exposure measured while performing power washing on swine farms were 0.94 mg m^{-3} for inhalable dust and 0.56 mg m^{-3} for respirable dust (Larsson et al. 2002). These exposures may result in respiratory symptoms and disease in the upper and lower airways on the human respiratory system (Zejda et al. 1993; Larsson et al. 1997; Wang et al. 1997). In another study, personal samples of endotoxin concentrations ranged from 5,401–180,864 endotoxin units (EUs) m^{-3} (O'Shaughnessy et al. 2012). These data suggest that swine farm workers experience occupational exposures to airborne dusts when performing power washing. Furthermore, dust increases as the number of swine per building increase which may cause increases in occupational exposures to dust.

General ventilation is an approach that can be used to control dust concentrations in swine buildings. However, ventilation design parameters in these buildings are based on the removal of moisture and heat generated by the animals, not on the mitigation of airborne dust (O'Shaughnessy et al. 2010). FFRs are a suitable PPE measure to reduce worker exposure to dust. However, few studies have demonstrated that the use of FFRs in swine farm environments can help reduce respiratory symptoms (Zejda et al. 1993; Popendorf et al. 1995; Dosman et al. 2000). Furthermore, to our knowledge, there is no study that addresses the BR of FFRs while performing power washing on a swine farm. Therefore, it is important to understand how FFRs perform in both laboratory and non-laboratory settings, where temperature and relative humidity are not strictly controlled.

To understand how FFRs and dust masks perform in laboratory and non-laboratory settings, the following research was conducted: 1) investigation of the effect of humidity and temperature combination on an approved FFR's performance in a laboratory setting, 2) evaluation of an uncertified dust mask's (UDM) performance against varying particle size in a laboratory setting, and 3) investigation of FFR's BR while performing power washing in non-laboratory setting, an enclosed building. The results of the three studies are aimed at protecting the health of workers that use respirators, and reducing workers' exposure to dust thus improving their long-term health.

In the remainder of Chapter 1 what is known about the relationship between power washing and workers' health will be described. In addition, the two major criteria used to evaluate FFR performance will be addressed; BR and efficiency of particle removal. Finally, the criteria used by NIOSH to certify a FFR will be explained.

Power Washing and Health Concerns

Power washing is used to clean surfaces in swine production buildings. A water spray generated when power washing aerosolizes material that has settled over flooring, gates, and other surfaces (O'Shaughnessy et al. 2012). Power washing is used in other occupational settings such as shipyards, automotive washing, storage facilities, and in livestock buildings. Performing the task of power washing can have negative outcomes that lead to various human health issues.

A few researchers have studied the effect of power washing on workers' health in swine farms. Larson et al. (2002) studied the health effects of human subjects exposed to aerosols generated during the power washing task among sixteen swine workers. Seven out of sixteen subjects used a respirator during the power washing task. Larson et al. (2002) identified that the aerosolized material generated by power washing was associated with an increased number of

inflammatory cells in the upper respiratory airways in subjects not wearing a respirator compared to subjects wearing the respirator.

An array of symptoms such as inflammation (acute and chronic) in the airways, occupational asthma, fever and headache can be caused by exposure to dust (Gustafsson, 1997). Organic dust commonly contains biologically active materials like microbes, endotoxins and pathogens (bacteria and viruses) that can lead to pulmonary symptoms such as congestion, coughing or wheezing, and sensitivity to dust. Also, an increased frequency of infections including colds, bronchitis, and pneumonia have been reported among workers exposed to organic dust (OSHA, Respiratory Protection, 2009). Donham et al. (1989) studied endotoxin exposure in a cohort of 54 swine farms in Sweden and the results showed that exposure to endotoxin concentration greater than 0.1 μg m^{-3} (1000 EU m^{-3}) is a risk factor for obstructive lung disease. Maximum allowable concentration suggested limits in indoor buildings for organic dust and endotoxin over an 8-hr work day was 10 mg m^{-3} and 0.08 μg m^{-3} (800 EU m^{-3}) respectively (Gustafsson, 1997). In addition, O'Shaughnessy et al. (2012) reported personal endotoxin exposures from 0.54 μg m^{-3} to 18.1 μg m^{-3} (5400-180,000 EU m^{-3}). These results indicate that workers performing power washing might be at greater risk of developing obstructive lung disease due to increased endotoxin exposure. Therefore, the use of respirators during the power washing procedure is recommended. Although the use of respirators has been shown to be beneficial during power washing (Larson et al. 2002), the power washing procedure might affect respirator performance. Power washing alters room humidity and increases dust concentration, which might impair respirator function by clogging the respirator and increasing BR through the respirator.

Respirator performance was not evaluated in any of these studies. A thorough review of the scientific literature did not reveal any studies that address respirator performance while performing power washing. In the next several sections, a review of the performance criteria for evaluating FFRs and a description of what is known about BR and filter efficiency in the research literature will be presented. Also, theory of filters filtration will be explained.

Breathing Resistance across Filters

Breathing resistance (BR) occurs when dust/dirt/particle mass deposits on the filter. BR across the filter is a function of the drag force applied to the air by the immobile fibers: it influences the energy required to move air through the filter (Raynor, 2008). BR, ΔP, can be calculated by the sum of pressure drops across the filter media, ΔP_{filter}, and the pressure drops across the particulate cake, ΔP_{cake}:

$$\Delta P = \Delta P_{filter} + \Delta P_{cake} \quad \text{Eq. 1}$$

Assuming the airflow through the media and particulate cake to be laminar and that they are superimposed on each other, then each component can be described by Darcy's law and written as

$$\Delta P_{filter} = K_1 V \quad \text{Eq. 2}$$

$$\Delta P_{cake} = K_2 V (M/A) \quad \text{Eq. 3}$$

where K_1 is the clean filter resistance, V is the filtration velocity, K_2 is the specific cake resistance, M is the mass deposited on the filter, and A is the filtration area of the filter. In theory, as the mass loading increases ΔP will increase linearly.

Previous research on high efficiency particulate air (HEPA) filters has demonstrated that ΔP does not always increase linearly with mass loading. Durham and Harrington (1971) observed a decrease in ΔP when fly ash particles were used at varying relative humidity (20-

60%). Ariman and Helfritch (1977) found a decrease in ΔP when relative humidity increased from 20% to 80% when fly ash, ground silica dust, and asphalt rock dust were used as a challenge aerosol. Novick and Higgins (1989) and Novick et al. (1990) observed a nonlinear increase in ΔP when sodium chloride (NaCl) aerosol from a high humidity stream was loaded on to HEPA filters. Smith et al. (1990) reported higher ΔP at higher humidity (65-99%) in HEPA filters. Ricketts et al. (1990) observed a significant ΔP increase in preloaded HEPA filters at a humidity greater than 70%. Grupta et al. (1993) observed a ΔP decrease with mass loading at higher humidity. Miguel (2003) reported a ΔP decrease with an increase in air humidity for Al_2O_3 particles, but an increase in ΔP was observed for NaCl particles. Data presented from previous research demonstrates that ΔP is influenced by aerosol loading particle hygroscopicity and the humidity in air (Miguel, 2003), but there are not clear results on whether relative humidity affects filter ΔP (Grupta et al. 1993) in HEPA filters used in respirators.

Studies have been conducted to evaluate BR of FFRs (Janssen, 2004; Roberge et al. 2010; Cho et al. 2011; Cho and Yoon, 2012). Janssen (2004) observed a statistically significant increase in BR when the FFR was challenged against cement dust, but below the pressure limit of 35 mm of H_2O as established by NIOSH (NIOSH, 1995). Cho et al. (2011) reported that BR increases faster when the filter was loaded with welding fume versus when loaded using NaCl aerosol in a laboratory setting. Cho and Yoon (2012) observed a BR increase when filters were loaded with welding fume in a field setting. However, neither of these studies evaluated the effects of relative humidity on the breathing resistance of the respirators. Only Roberge et al. (2010) investigated the effect of exhaled moisture on breathing resistance of N95 FFRs. Under ambient conditions, a BR increase of 3% was observed. However, this study did not look at

different humidity conditions outside the FFR. Therefore, it is still not clear how ambient humidity will affect breathing resistance of respirators.

BR is an important factor when studying whether workers will use their FFRs and as a criterion used to replace FFRs. The Occupational Safety and Health Administration (OSHA) recommends that FFRs should be replaced when breathing becomes difficult, the FFRs become dirty or they are physically damaged (OSHA, 2009). When the work activity increases, breathing rate and tidal volume will rise (Roberge et al. 2010). With an increase in breathing rate, BR through the mask increases. The increase in BR results in a greater physical effort to breathe through the FFR. As a result, it is possible that workers may be less likely to use the FFR due to the increased resistance and will thus be exposed to the contaminant.

As explained previously, research on HEPA filters demonstrated that the effect of humidity on the behavior of ΔP across the filter can be attributed to an increase in the particle-to-particle adhesive forces as the air humidity increases (Gupta et al. 1993). High moisture on FFRs will block the openings between the filter fibers thereby increasing the BR through the FFRs (Belkin, 1996; Mardimae et al. 2006). Furthermore, condensation of exhaled air will form when air temperature outside the body is low or when moisture is high (Shaviv, 2006). FFRs' BR is expected to increase when the air passes through the condensed water vapor on the filter fiber. Therefore, if BR is high it can be expected that the worker will not use the respirator properly and the worker will be exposed to the hazard.

Efficiency across Filters

Efficiency is a measure to describe how well a filter removes particles from air. Efficiency is the fraction of particles entering a filter that are collected and is influenced strongly by particle diameter (Raynor, 2008). In theory, respirators that remove all the particles from the

airstream have an efficiency of 100%.There are five physical mechanisms by which filters remove particles from air: interception, inertial impaction, diffusion, gravitational settling, and electrostatic attraction. These mechanisms are based on single fiber theory and have been explained previously (Stafford & Ettinger, 1972; Richardson, Eshbaugh, & Hofacre, 2006; Raynor, 2008) and texts (Hinds, 1999; Marijnissen & Gradon, 2010).

Interception happens when particles in an airstream come within one particle radius of the surface of the fiber and are captured. Impaction occurs when the particle with inertia cannot stay in the airstream flowing around the fiber and therefore hits the fiber. Impaction is most effective for larger particles and is enhanced by higher particle velocities. Small particles that do not follow the airstream because of random (Brownian) motion are captured by diffusion when traveling near the fiber. In addition, capture by diffusion increases as the particle size decreases and as the time the particle spends in the filter area increases. The gravitational settling mechanism is due to the force of gravity and the associated settling velocity of the particle, which causes it to go across the airstream and reach the fiber. Electrostatic attraction is typically an improvement to mechanical filtration, by improving filtration efficiency of particles without affecting BR when compared with an uncharged filter of similar composition. By a physical force, Coulomb force, the electric charge in the fiber will attract the particle with an opposite electric charge. Also, a neutral particle is captured when an electric charge rearrangement (polarization) occurs in the particle induced by the electric fields within the filter fibers (Hinds, 1999; Marijnissen & Gradon, 2010). In order to assure the removal of different particle sizes by the respirator, all of the above mentioned mechanisms are considered when fibers are mingled to build the respirator. Particles greater than 1 μm are primarily captured by impaction and interception, and particles smaller than 0.01 μm are primarily captured by diffusion.

Filter efficiency, E, through the respirator can be calculated as a ratio of the number concentration of particles removed from the airstream that passes through the respirator:

$$E = \left(1 - \frac{C_{in}}{C_{out}}\right) \times 100 \qquad \text{Eq. 4}$$

where C_{in} is the number concentration of particles penetrating through, and C_{out} is the number concentration of particles outside the respirator. In theory, respirator efficiency will be higher as the dust cake on the filter media builds up.

Importantly, respirator efficiency can be affected by numerous conditions such as air velocity, particle size diameter, fiber diameter, and humidity (Davies, 1973; Dullien, 1989; Haghighat et al. 2012). Previous work has shown the effects of humidity on the efficiency across the filters (Miguel, 2003; Durham & Harington, 1971). Miguel (2003) found that filter efficiency decreases as humidity increases when tested against alumina (Al_2O_3) aerosol. In contrast, Durham & Harington (1971) found that filter efficiency increases with increasing humidity for different filter fibers when challenged against fly ash. The apparent contradictions in the effects of humidity on filter efficiency require additional analysis to inform respirator effectiveness in workplaces where humidity is greater than 90 %.

Approval of FFRs and Dust Masks

Respirators are filters composed of a mesh of fibers with a distinct fiber diameter and material that remove particles from the air the user is breathing (NIOSH, 1995). The National Institute for Occupational Safety and Health (NIOSH) approves FFRs to ensure they provide a minimum level of protection against particle dust in the workplace. The qualifications to approve FFRs are in accordance to the Code of Federal Regulation (Title 42 CFR Part 84).

A total of nine classes of NIOSH-approved FFRs are available. A combination of three letters (N, R, and P) and three numbers (95, 99, and 100) are used to designate FFR class type. N

stands for “not resistant to oil”, R stands for “somewhat resistant to oil”, and P stands for “strongly resistant to oil” (NIOSH, 1995). The 95, 99, and 100 classifications are referring the FFR’s filtration efficiency under certain challenge conditions (NIOSH, 1995).

A NaCl aerosol test is used to certify N-class FFRs, and a dioctyl phthalate aerosol test is used to certify R-class and P-class FFRs (NIOSH, 1995). An N-95 class means the FFR is at least 95% effective against the sodium chloride aerosol test. A P-100 class means the FFR is at least 99.97% effective against the dioctyl phthalate aerosol test. The FFR efficiency is evaluated at the maximum particle size that pass through the FFR

BR is another criteria used by NIOSH to pass or fail a respirator (NIOSH, 1995). The BR test used by NIOSH recommends 35 mm of H_2O as the maximum inhalation breathing resistance and 25 mm of H_2O as the maximum exhalation BR to certify FFRs measured at constant one-direction airflow of 85 L min^{-1} (NIOSH, 2005). However, it is important to understand the effects of a two directional airflow on FFR BR.

FFR performance is measured by testing the FFR at a constant and high flow in one direction from the outside to the inside of the mask. However, when FFR users breathe, air moves in two directions, inhalation and exhalation flows that are similar to a cyclic flow (Johnson, 1993). Despite a large amount of research associated with evaluating FFRs, few studies have been conducted to determine FFR performance under cyclic flow (Cho et. al. 2013; Cho et. al. 2010; Eshbaugh et. al. 2009; Grinshpun et. al. 2009). Cho (2013) found that filter penetration was below 5% for the N95 respirators tested. Cho (2010) found that filter penetration decreased with increasing particle size. This result was consistent with classic filtration theory. Eshbaugh et al. (2009) found that particle capture efficiency decreased with an increase in flow rate. Grinshpun et al. (2009) demonstrated that particles in the range between 0.04-1 μm

penetrated the filter media less than 1% in one N95 FFR. However, these studies did not look at the effect of humidity on the FFR performance. Therefore, further research is needed to understand how humidity will affect breathing resistance and efficiency of respirators under cyclic flow.

Uncertified dust masks (UDMs) are dust masks not approved by NIOSH because they do not meet NIOSH requirements (Title 42, Code of Federal Regulations, Part 84) for protection, or are not sent to the NPPTL for certification. However, UDMs are advertised by companies or manufacturers for protection against pollen, dust, diesel fumes, molds, smoke, and other particles. Although some UDMs have one strap, some have two straps and look similar to FFRs it is unclear how protective these UDMs are to workers as there has been no published research on UDM performance.

Breathing resistance, filter efficiency and total inward leakage were evaluated in the past to determine some UDMs' performance. Cherrie et al. (1987) studied the efficiency of UDMs against cement dust that had a mass median diameter (MMD) of 3 μm. Six subjects wore seven different UDMs and performed a series of tasks simulating light work while wearing the UDMs. Three of the UDMs were cup shaped, two were semi-rigid plastic face pieces, one was a "flat sheet", and one was a flexible plastic skeleton face-piece. The results indicated that particle penetration ranged between 1.5% - 36%. Wake & Brown (1988) evaluated the filtration efficiency and BR of UDMs against limestone and cement dust. A test apparatus was used to evaluate 17 UDMs classified into four categories as "cup", "face pad", "soft fabric", and "supported pad". Initial BR for the UDMs varied from 0.286 mm H_2O to 4.05 mm H_2O. The penetration test was performed at a flow rate of 30 L min^{-1} and at flow rate equivalent to 150 L min^{-1} which are lower and higher than the airflow used by NIOSH to evaluate FFRs of

85 L min^{-1}. Their results demonstrated that UDMs penetration ranged between 1% and 55% against limestone dust.

The results of these studies suggest that UDM performance is not as consistent when compared to FFRs. However, the Cherrie et al. (1987) study determined that UDMs have a good efficiency against particles with a median diameter of 3 µm, which is 29% smaller than the particles found on swine farms (Reynolds et al. 2009). With an expected lower initial breathing resistance it will be easier to breathe through the UDMs and therefore workers may be more likely to use the mask for a longer time period, which would reduce their exposure to dust until engineering controls can be implemented.

Total Inward Leakage

NIOSH proposed on October 30, 2009 to establish Total Inward Leakage (TIL) requirements under the 42 CFR Part 84 for half-mask air-purifying particulate respirators, including FFRs. Although TIL is not a requirement to pass or fail the respirator approval test, it is used during respirator fit testing to consider face seal leakage. TIL testing quantifies the respirator's ability to fit the facial dimensions of individuals to ensure the respirator fits properly.

Shortcomings of the Literature

There are key issues that need to be studied with attention to N95 FFRs and UDMs use in the workplace. N95 FFRs are certified in a controlled lab setting, but work environments in which they are used differ from the lab settings. The simulated work conditions performed in a laboratory setting needs to be expanded to represent similar work tasks and environmental conditions in workplaces where FFRs are used. Many work operations have varying temperature and humidity conditions. Identifying and characterizing these environmental conditions is

necessary for improving FFRs design and for a more efficient protection of workers who are exposed to particulates in air.

More studies are needed to evaluate commercially available UDMs used in workplaces. Previous studies showed that UDMs have limitations with regard to the efficiency they provide. However, new technologies or designs have been developed and their limitations are not well known. Studying the UDMs to identify their limitations is essential to determine the feasibility as a way to reduce exposure to dust.

Specific Aims

The work presented in this doctoral dissertation attempts to reduce the previous shortcomings of the literature by increasing knowledge with regard to respirator performance in the workplace. The overall goal is to protect the health of workers that are required to use respirators. Despite a significant amount of research assessing FFRs performance against different types of aerosols, few studies have been conducted to determine whether moisture affects FFR performance. The central hypothesis is that workers avoid wearing respirators because breathing through them becomes difficult, especially in high humidity conditions. The following three aims were established to accomplish that goal:

Aim 1. Determine the effect of different air environmental conditions on the breathing resistance and particle penetration of N95 FFRs.

Aim 2. Determine the maximum particle penetration of UDMs and evaluate the increase in breathing resistance with particle loading over time to compare breathing resistance between UDMs and FFRs.

Aim 3. Evaluate N95 FFRs' breathing resistance while performing pressure washing in an enclosed building.

CHAPTER II

THE EFFECT OF SIMULATED AIR CONDITIONS ON N95 FILTERING FACE-PIECE RESPIRATORS PERFORMANCE

Abstract

The objective of this study was to determine the effect of simulated air environmental conditions on the particle penetration and the breathing resistance of two N95 filtering face-piece respirators (FFR) models. The particle penetration and breathing resistance of the respirators were evaluated in a test system developed to mimic inhalation and exhalation breathing, while relative humidity and temperature were modified. Breathing resistance was measured over 120 min using a calibrated pressure transducer under four different temperature and relative humidity conditions. Particle penetration was evaluated before and after the breathing resistance test using a sodium chloride aerosol measured with a scanning mobility particle sizer. Results demonstrated that increasing relative humidity and lowering external temperature caused significant increases in breathing resistance ($p < 0.001$). However, these same conditions did not influence the penetration or most penetrating particle size of the tested FFRs. The increase in breathing resistance varied by FFR model suggesting that some FFR media are less influenced by high relative humidity than other media models.

Introduction

Filtering face-piece respirators (FFR) are well-recognized personal protective equipment (PPE) used by workers to provide protection against airborne particulate in a variety of occupational settings (NIOSH, 1995). An estimated three million workers wear FFRs throughout the United States in an estimated 200,000 workplaces (Doney et al. 2005). Agriculture, manufacturing, construction, and mining are some of the industries that use FFRs (OSHA, 2014).

FFRs worn correctly will protect the wearer in many workplace settings and can prevent acute or chronic health symptoms to the wearer.

Efficiency of particle removal and breathing resistance (BR) are the principal criteria for measuring FFR performance (Friedlander, 1958). The National Personal Protective Technology Laboratory (NPPTL) tests FFRs using the method described in the Code of Federal Regulations (Title 42 CFR Part 84) (NIOSH, 1995). An N95 FFR, the most commonly used FFR, will remove at least 95% of particles in the air that the user is breathing. The NPPTL tests FFRs efficiency and BR in a laboratory setting where the variables of temperature (77°F), relative humidity (30%) and one-direction airflow (85 L min^{-1}) are controlled. NIOSH certifies FFRs when the inhalation BR is less than 35 mm of H_2O and the exhalation BR is less than 25 mm of H_2O measured at constant one-direction airflow of 85 L min^{-1} (NIOSH, 2005). However, FFR efficiency and BR can be affected by numerous conditions such as air velocity, particle size diameter, fiber diameter, and humidity (Johnson, 1993; Cho et al. 2010; Cho et al. 2013). Furthermore, environmental conditions where FFRs may be used, for example when power washing which creates a high humidity environment that can differ from the laboratory conditions where FFRs are certified.

FFR efficiency and BR are measured by testing the FFR with a constant high air flow from the outside to the inside of the FFR. However, when FFR users breathe, air moves in two directions, inhalation and exhalation flows that are similar to a cyclic flow (Johnson, 1993). Despite a large amount of research associated with evaluating FFRs, few studies have been conducted to determine FFRs efficiency under cyclic flow (Cho et. al. 2013; Cho et. al. 2010; Eshbaugh et. al. 2009; Grinshpun et al. 2009). Cho (2013) found that filter penetration was below 5% for the N95 respirators tested as required for that type of respirator. Cho (2010) demonstrated

that filter penetration decreased with increasing particle size (0.7-4 μm). Eshbaugh et al. (2009) found that particle capture efficiency decreased with an increase in air flow rate. Grinshpun et al. (2009) demonstrated that particles in the range between 0.04-1 μm penetrated the filter media less than 1% in one N95 FFR. However, these studies did not evaluate the effect of humidity on FFR performance. Therefore, it is not clear how humidity will affect efficiency and BR of FFRs under cyclic flow.

Various studies have been conducted to evaluate BR of FFRs (Janssen, 2004; Roberge et al. 2010; Cho et al. 2011; Cho and Yoon, 2012). Janssen (2004) observed a statistically significant increase in BR when the FFR was challenged against cement dust, but below the pressure limit established by NIOSH (Grinshup et al. 2009). Cho et al. (2011) reported that BR increases faster when the filter was loaded with welding fume versus when loaded using NaCl aerosol in a laboratory setting. Cho and Yoon (2012) observed a BR increase when filters were loaded with welding fume in a field setting. However, neither of these studies evaluated the effects of humidity on the BR of the FFRs. Only Roberge et al. (2010) investigated the effect of exhaled moisture on BR of N95 FFRs. Under ambient conditions, the BR increase of 3% was observed. However, that study did not look at different humidity conditions upstream the FFR. For example, air condensation will occur when air temperature outside the body is lower than the body temperature or when moisture is high (Shaviv, 2006). Therefore, it is still not clear how ambient humidity will affect BR of FFRs.

Previous work has shown the effects of humidity on the efficiency across HEPA filters (Miguel, 2003; Durham & Harington, 1971). Miguel (2003) found that filter efficiency decreases as humidity increases when tested against alumina (Al_2O_3) aerosol. In addition, Durham & Harington (1971) found that filter efficiency increases with increasing humidity for different

filter fibers when challenged with fly ash. The apparent contradictions in the effects of humidity on filter efficiency require additional analysis to provide an assessment when respirators are used in high humidity workplaces.

Additional research on respirator performance is needed for several reasons. As mentioned above, human breathing consists of inhalation and exhalation airflow, not constant one-direction airflow as dictated in the NIOSH method for assessing FFRs' filtration performance (NIOSH, 2005). Also, several studies that have simulated breathing to test the efficiency of FFRs did not take into account humidity in exhaled air (Rengasamy, 2011; Cho et al. 2010; Eshbaugh et al. 2009). Knowing the effects of air humidity upstream and downstream the FFR is an important factor for improving FFRs design and for a more efficient protection of workers who are exposed to particulates in high humidity workplaces. The goal of this study was to determine the effect of air temperature and humidity on the BR and particle penetration of N95 FFRs. The effect of air humidity on the BR was evaluated using a novel cyclic flow system. The effect of changes to the most penetrating particle size (MPPS) and the amount of mass gained of the FFRs were also characterized. Also, BR, water retention and moisture regain evaluation of individual FFR layers were performed.

Methods

Filtering Face-piece Respirators (FFRs) Characteristics

Two models of N95 respirators were selected for use in this study because they are commonly used in occupational settings and have different physical characteristics that could make them perform differently across temperature and relative humidity conditions (Fig. 1). FFR 1 (3M 8510, St. Paul, MN) was a three-layer respirator with a rigid external layer followed by a middle layer of electret filter material and a thin internal layer. FFR 2 (Moldex 2200, Culver

City, CA) was a two-layer respirator with a flexible mesh over the external electret filter material followed by a thin internal layer similar to that of FFR 1. Table I summarizes the physical characteristics of the tested FFRs. The filters were weighed in a balance with a sensitivity of 1 mg (Mettler PE 360, Mettler-Toledo LLC, Columbus, OH). The thickness of each layer, L, was measured using a digital caliper (Neiko 01407A). Scanning electron microscopy (SEM) (Hitachi S-4800, Hitachi High Technologies America, Inc., Schaumburg, IL) of the FFRs were used to analyze fiber diameter. Fiber diameter and surface area were measured using ImageJ software (National Institutes of Health (NIH), Bethesda, MD). The method described by Balazy et al. (2006) was used to calculate packing density (α).

Table I. FFRs characteristics (Mean ± S. D.)

FFR Model	Mass (g)	Thickness (mm)	Fiber diameter (μm)	Surface area (m^2)	Surface density ($g\ m^{-2}$)	Packing density (α)
FFR 1				0.0163		
External layer	3.53 ± 0.12	2.27 ± 0.28	22.1 ± 5.3		217.30	0.104
Middle layer	2.54 ± 0.17	1.77 ± 0.05	5.4 ± 3.2		156.11	0.096
Internal layer	0.55 ± 0.03	0.36 ± 0.08	15.4 ± 1.3		33.55	0.101
FFR 2				0.0188		
External layer	1.19 ± 0.01	1.30 ± 0.19	5.1 ± 4.6		63.01	0.053
Internal layer	0.53 ± 0.02	0.61 ± 0.11	15.5 ± 1.2		28.33	0.051

Figure 1. Image of FFRs used in this study

Test System

Two test system were designed to measure FFR particle penetration and BR under cyclic flow. Fig.2 shows the experimental setup used for measuring particle penetration and Fig. 3 shows the experimental setup used for measuring BR. A male full round plastic manikin head was used to hold the FFR while performing the particle penetration and BR tests. The manikin head was placed in a 0.055-m^3 acrylic plastic, sealed chamber. As shown in Fig. 2, the manikin head contained a pipe protruding from the mouth area to the back of the head. An additional pipe was used to carry air outside of the chamber. A four-way connector was used to divide the airflow direction, as shown in Fig. 3. A pipe connected a vacuum pump to one side of the four-way connector. For the BR test, another pipe was used to connect an air pump to another side of the four-way connector. This side was blocked for the particle penetration test. The available side of the four-way connector was used to insert a tube to the inside of the FFR for sampling. A second piece of tube was inserted into the chamber and placed beside the manikin head for sampling outside the FFR. Depending on the test, these two tubes were connected to a three-way valve (Fig. 2) or to the differential pressure sensor (Fig. 3). Air filters were connected to an inlet hole in the side of the chamber to remove particles from the air that entered the chamber.

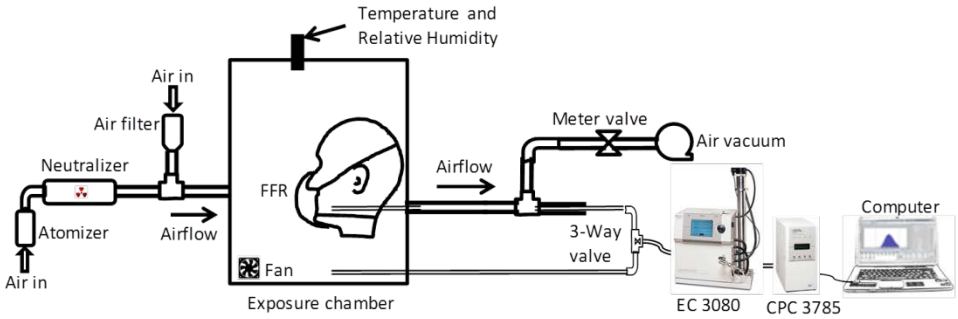

Figure 2. Schematic diagram of the test system used to determine NaCl particle penetration through an N95 FFR.

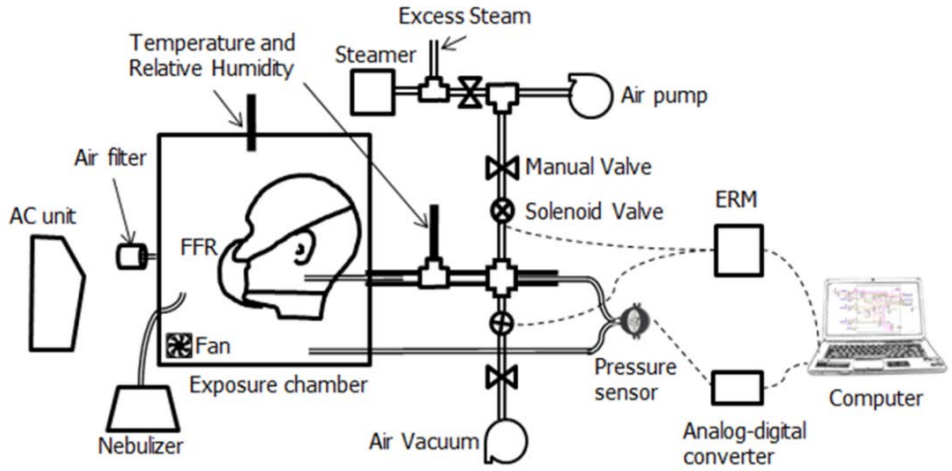

Figure 3. Experimental set up of the test system used to determine BR of an N95 FFR

Penetration Testing

Particle penetration was carried out in the chamber using a NaCl aerosol generated from a 2% solution applied to a nebulizer, as specified by NIOSH to certify N95 FFRs (42 CFR 84.181). The environmental conditions during both particle penetration tests (initial and final) were maintained at 77°F and 30% relative humidity. The aerosol was charge-neutralized with an ^{85}Kr source (Model 3077A, TSI Inc., St. Paul, MN). Fig. 2 shows a schematic of the experimental set-up that was used to measure particle penetration through the FFR. The generated aerosol was passed through the charge neutralizer, was diluted with filtered air and was sent to the inside of the chamber to generate a steady-state concentration. The aerosol generation was started and allowed to stabilize for five min. A small fan inside the chamber was

used to mix the aerosol inside the chamber. The penetration test required a continuous airflow at 85 L min^{-1} to be pulled through the FFR with a vacuum pump. A flowmeter (Model RMC-104, Dwyer Instrument Inc., Michigan City, IN) and a metered valve were placed between the chamber and the vacuum pump to establish the operational airflow. Airflow calibration was conducted with a calibrator (Model 4046, TSI Inc., Shoreview, MN) before each test.

The particle count and size distribution were measured with a scanning mobility particle sizer (SMPS) consisting of electrostatic classifier (Model 3080, TSI Inc., Shoreview, MN) in combination with a condensation particle counter (CPC) (Model 3785, TSI Inc., Shoreview, MN). The SMPS counted particles within 103 channels ranging between 7 – 289 nm. As shown in Fig. 2, the sample line to the SMPS was evenly split to enable sampling of particles upstream and downstream in the central portion of the FFR. A valve was manually turned to direct flow from one sample line to the other. The particle penetration was determined as a ratio of the particle concentration inside (C_{in}) the FFR and outside (C_{out}) the FFR for every SMPS size channel.

$$P(\%) = \frac{C_{in}}{C_{out}} \times 100 \qquad \text{Eq. 5}$$

During each trial, particle concentrations by size were measured with the SMPS three times in succession outside the FFR, then three times inside the FFR, and then again three times outside the FFR. C_{in} was calculated as the average of three measurements inside the FFR and C_{out} was the average of six measurements outside the FFR. The second set of outside measurements were taken to ensure the aerosol concentration remained steady during each test; if the average of the two outside aerosol measurements varied by more than 10%, that trial was rejected and re-conducted (Balazy et al. 2006). Given average penetration for all size channels, the maximum

penetration was obtained as well the median diameter of the channel containing the maximum penetration, reported as the MPPS for the FFR under the tested conditions.

Breathing Resistance Testing

Inhalation BR was evaluated using cyclic flow. Fig. 3 provides a schematic of the experimental set-up that was used to measure BR through the FFR. Compressed air was conditioned to achieve 95% relative humidity and 98°F to represent *exhaled air* from the inside to the outside of the FFR. A commercial steamer (Wagner 705, Plymouth, MN) supplied with distilled water was used to achieve both of these exhaled air conditions by producing warm, moist air that was controlled by venting a majority of the flow from the steamer, which was outside the chamber (Fig. 3). Temperature and relative humidity were monitored with a factory calibrated environmental sensor (Q-Trak, TSI, Shoreview, MN).

To simulate inhaled air, a vacuum pump pulled air from outside to the inside of the FFR at 55 L min^{-1}, a flow rate considered to be heavy breathing (Silverman et al. 1951; Stafford et al. 1973). Airflow changes, between inhalation and exhalation occurred every 1.25 seconds (respiratory rate of 24 breaths min^{-1}) by periodically activating solenoid valves (DS6013, Burkert Inc., Irvine, CA; AVS-312-120A, Nitra Pneumatics, Cumming, GA). The solenoid valves were connected to an electromechanical relay module connected to a computer. The LabVIEW (Ver. 2010, National Instruments, Chicago, IL), software program was used to operate the solenoid valves to switch between inhalation and exhalation modes while maintaining the airflow at 55 L min^{-1}.

Environmental conditions for inhaled air were varied. As shown in Table II, simulated exhaled air conditions were compared to a control scenario in which both inhaled and exhaled air were set to room conditions (70°F, 40% RH). Inhaled air was conditioned with a combination of

a portable air conditioner unit (PH3-12R-03, Soleus International Inc., City of Industry, CA) and a commercial nebulizer (Ultra-Neb 99, DeVilbiss Healthcare LLC, Somerset, PA). Distilled water was used in the nebulizer to produce moist air outside the filter as shown in Fig. 3 and the AC unit produced an air temperature below room conditions (50°F). The air inside the chamber was monitored with the Q-Trak.

A calibrated differential pressure sensor (Series 646B, Dwyer Instruments Inc., Michigan City, IN) measured BR across the FFR. As shown in Fig. 3, the sensor was connected with tubing to upstream and downstream to the central portion of the FFR. The pressure sensor range was 0-2.5 inches of H_2O via proportional voltage output of 0.5-4.5 volts and was connected to an analog-to-digital converter to measure the voltage with a full scale accuracy of ± 2% (0.05 in H_2O). During each trial, an initial BR measurement was made during the first minute of operation and then every 30 minutes over the 120-min trial period. During each measurement, the switching mechanism was stopped and BR was measured every one second for five seconds while operating with inhalation flow only and an average computed for the four measurements taken. Data were exported to Minitab® (Ver. 17, Minitab Inc., State College, PA) to perform the statistical analysis.

Experimental Design

Tests were conducted to determine how air humidity affects FFR particle penetration and BR under cyclic flow and various simulated air conditions. In general, FFRs were weighed before being sealed onto the manikin head. Then, an initial NaCl aerosol penetration test was performed following NIOSH certification protocol (42 CFR 84.181) modified to not include pre-conditioning the FFR. Next, a BR test under cyclic flow was performed for 120 min and under a specific set of environmental conditions as shown in Table II. Conditions were tested always in

order from Condition 0 to Condition 3. After 120 min, a second ("final") NaCl aerosol penetration test was performed. Finally, the FFR was removed from the manikin head and reweighed. The difference between initial and final weight was referred to as the mass gained (MG).

Condition 0 served as a control environment consisting of typical room temperature and relative humidity for both the inhalation and exhalation air. Condition 1 was a modification of Condition 0 by simulating human exhaled breath consisting of air at 98°F and 95% RH (Shaviv, 2006). Condition 2 was a modification of Condition 1 to include cool, humid inhalation air to simulate situations that may enhance water absorption by the filter media. Condition 3 was similar to Condition 2 except the humidity was increased just to the point of saturation (100% RH) to simulate conditions when condensation may occur. Five trials per simulated condition per FFR were completed.

Table II. Designed conditions during BR test (Mean ± S. D.)

	Inhalation		Exhalation	
Condition	T (°F)	RH (%)	T (°F)	RH (%)
0	72.4 ± 1.8	38.9 ± 3.9	72.4 ± 1.8	38.9 ± 3.9
1	77.2 ± 3.1	48.4 ± 9.3	94.1 ± 4.3	94.4 ± 5.3
2	59.7 ± 2.6	97.2 ± 2.7	94.9 ± 3.5	97.0 ± 4.3
3	63.8 ± 4.5	99.3 ± 1.8	94.0 ± 5.2	97.1 ± 3.2

Evaluation of Unused FFR Individual Layers

Since the tested N95 FFRs were multilayered, FFR layers were tested individually to evaluate BR, water retention value (WRV) and moisture regain value (MRV) by layer. It was of interest to us to determine differences at the filter layer level primarily with regard to BR. The WRV provides an indication of the amount of moisture absorbed into, and retained within, the filter fibers (Siroka et al. 2008). The MRV is a measure of the moisture that is adsorbed on the

surface of the filter fibers (Kongdee et al. 2004). SEM images were also obtained to examine the composition of the FFRs external layers visually.

BR of Individual FFR Layer

BR of unused FFR individual layers were measured by sealing a section of the filter layer and passing air with 95% RH using a constant flow equivalent to 55 L min^{-1}. An apparatus was developed for this purpose that consisted of a stainless-steel Tri-Clover clamp apparatus. This apparatus consisted of two 3.8 cm dia. flat circular pieces with a 1.6 cm dia. central hole that were clamped together to hold a 2.5-cm dia. piece of filter layer securely while air flowed through the center hole and through the area of the filter layer covering the hole. Pressure taps were applied on either side of the clamp apparatus to measure BR for 30 min in triplicate.

Water Retention Value (WRV)

The WRV of each filter layer was determined following the methods described by Kongdee et al. (2003) and Siroka et al. (2008). Filter layer sections were immersed in deionized water at room temperature for 24 h. Then, the filter layer sections were centrifuged at 4000g for 10 min to remove excess water and weighed (W_w) in a microbalance. The filter layer sections were then dried in an oven at 105°C for 4 h, and reweighed (W_d). WRV was calculated using the following equation

$$WRV = \frac{W_w - W_d}{W_d} \quad \text{Eq. 6}$$

Moisture Regain Value (MRV)

The MRV of each filter layer was determined following the method described in Kongdee et al. (2003). Filter layer sections were conditioned in a standard atmosphere of 85% RH at room temperature for 48 h and then weighed (W_C). The sections were then dried in an oven at 105°C for 4 h and reweighed (W_D). MRV was calculated using the following equation.

$$MRV = \frac{W_C - W_D}{W_D} \quad \text{Eq. 7}$$

Statistical Analysis

Three statistical analyses were performed to assess differences in the MPPS, percentage penetration, BR, and MR between and within FFRs. The first analysis involved a comparison between the mean of initial values for all conditions between the FFRs. Initial values were those recorded within 1 min of the start of a trial. The second analysis compared initial and final values within FFRs, where final values were those recorded at the end of the 120-min trial. The third analysis was conducted to determine differences between Condition 0 and Conditions 1, 2, and 3 as defined in Table II. All comparisons were conducted as two-sample T-tests with statistical significance accepted at the $\alpha = 0.05$ level.

Results

Data sets were tested for normality using the Anderson-Darling test and found to be normally distributed. The mean initial and final values of the 20 total samples taken for all four conditions are presented in Table III. Data is separated to compare both within and between FFRs.

Table III. Values of most penetrating particle size (MPPS), penetration (P), breathing resistance (BR), and mass for all conditions (Mean ± S. D.)

	MPPS, nm	P, %	BR, mm H_2O	Mass, g
Between FFRs[1]				
FFR 1 Initial	41.7 ± 4.7	2.8 ± 0.7	11.2 ± 0.8	10.6 ± 0.2
FFR 2 Initial	**50.5** ± 5.4	**5.1** ± 1.6	**13.0** ± 0.8	**14.2** ± 0.4
Within FFR[2]				
FFR 1 Final	43.5 ± 3.8	3.1 ± 1.1	**13.1** ± 1.8	**12.0** ± 1.2
FFR 2 Final	52.4 ± 7.6	5.3 ± 2.0	**16.8** ± 3.3	**15.8** ± 1.4

[1]Bolded values are significantly different ($\alpha < 0.05$) from comparable value obtained for FFR 1.
[2]Bolded values are significantly different ($\alpha < 0.05$) from the comparable initial value.

Table IV provides results separated by test condition. Displayed are the mean values for the five samples taken for each condition at the end of each trial.

Table IV. Final values of the most penetrating particle size (MPPS), penetration (P), breathing resistance (BR), and mass gained (MG) for each respirator and each test condition (Mean ± S. D.)

	Test Conditions			
FFR models	0	1	2	3
FFR 1				
MPPS, nm	40.6 ± 2.5	43.0 ± 2.4	44.3 ± 3.0	46.3 ± 5.1
P, %	2.5 ± 0.9	2.9 ± 0.7	2.6 ± 0.2	4.2 ± 1.4
BR, mm H_2O	11.7 ± 1.0	13.5 ± 1.6	**14.3**[1] ± 1.6	13.0 ± 2.4
MG, g	0.003 ± 0.085	**1.05** ± 0.61	**1.74** ± 0.73	**2.82** ± 0.98
FFR 2				
MPPS, nm	54.0 ± 7.3	51.3 ± 11.1	49.1 ± 5.1	55.1 ± 6.5
P, %	3.8 ± 0.7	**7.2** ± 1.7	3.8 ± 0.4	**6.5** ± 1.7
BR, mm H_2O	13.5 ± 0.3	**15.0** ± 0.7	**17.1** ± 1.2	**21.6** ± 1.1
MG, g	0.059 ± 0.034	**1.44** ± 0.71	**2.05** ± 0.32	**2.84** ± 1.02

[1]Bolded values are significantly different ($\alpha < 0.05$) from comparable value obtained under Condition 0.

Most Penetrating Particle Size

The initial mean MPPS value for FFR 1 (41.7 nm) for all conditions was significantly different than the initial mean MPPS value for FFR 2 (50.5 nm) ($p < 0.001$). The final mean

MPPS values did not differ from the initial MPPS values within either FFR model [FFR 1 ($p = 0.17$) and FFR 2 ($p = 0.16$)]. Comparisons of the final MPPS between Condition 0 and all other conditions within FFR model were not significantly different for any condition.

Penetration

The mean penetration values for the FFR 1 were below the NIOSH certification limit. However, the mean penetration values obtained for FFR 2 exceeded the 5% NIOSH certification limit for two test conditions (Table IV). The initial mean penetration value for FFR 1 (2.8%) was significantly different from FFR 2 (5.1%) ($p < 0.001$).

Fig. 4 shows the difference between the final and initial penetration measurements for the two FFRs for each simulated test condition. Aerosol penetration increased between the initial and final tests for all conditions for both FFRs except Condition 2 for FFR 1 and Condition 0 for FFR B (Fig. 4). However, the average final mean penetration values (Table III) for both FFR models did not differ significantly from the average initial penetration values within FFR model [FFR 1 ($p = 0.34$) and FFR 2 ($p = 0.69$)] (Table IV).

Comparisons of the final penetrations within FFR 2 and between conditions were significantly different between Condition 0 and Conditions 1 and 3 for FFR 2 (Table IV). The similar comparisons between conditions for FFR 1 did not result in significant differences.

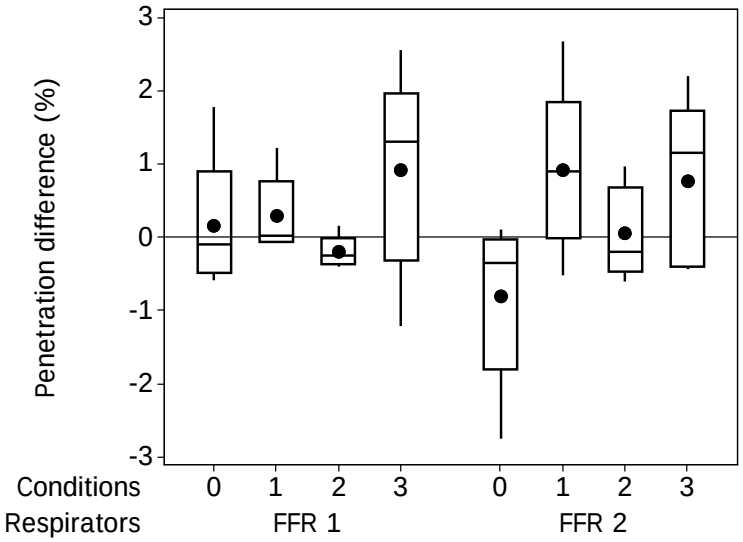

Figure 4. Difference in particle penetration for two N95 FFRs. (Error bars indicate the range of the difference).

Breathing Resistance

The initial mean BR for FFR 1 (11.2 mm H_2O) was significantly different from FFR 2 (13.0 mm H_2O) ($p < 0.001$). The final mean BR values (Table III) for both FFR models differ from and were greater than the initial BR values within FFR model ($p < 0.001$). Comparisons of BR within the FFRs and between conditions showed significant differences between Condition 0 and Condition 2 for FFR 1 and between Condition 0 and all other conditions for FFR 2 (Table IV).

After 120 min of testing, none of the FFR's exceeded the NIOSH certification limit for BR of 35 mm H_2O (Table IV). A box plot of the differences between the final and initial BR values for both FFRs tested for the four different simulated test conditions is given in Fig. 5. Given these results the BR after an 8-hr at these test conditions would be expected to be between 20 – 24 mm H_2O for FFR 1 and between 22 – 49 mm H_2O for FFR 2.

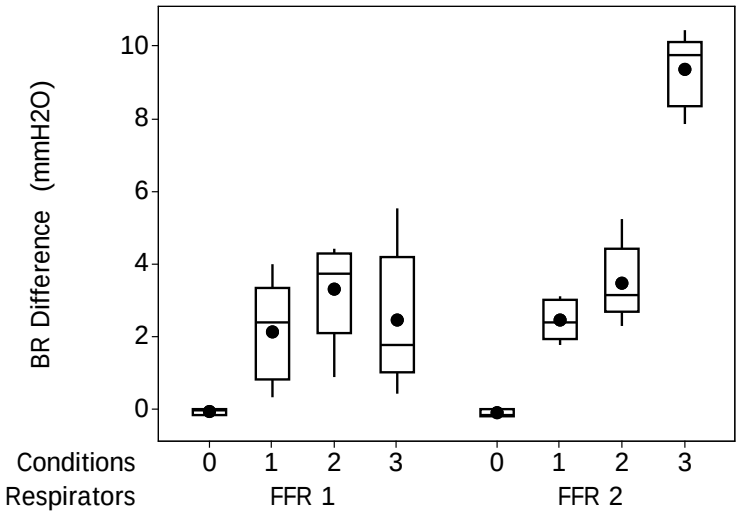

Figure 5. Difference in breathing resistance for two N95 FFRs (Error bars indicate the range of the difference).

Mass Gained

The initial mean mass value for FFR 1 (10.6 g) was significantly different from FFR 2 (14.2 g) ($p < 0.001$) (Table IV). The final mean mass values (Table III) for both FFR models was greater than the initial mass values within FFR model ($p < 0.001$) (Table IV). Comparisons of MG within the FFRs and between conditions showed significant increase in moisture retention between Condition 0 and all other conditions for both FFRs (Table IV).

A box plot was constructed of the difference between the final and initial MG values for the two FFRs tested against the four different simulated air conditions (Fig. 6). As shown in Fig. 6, MG increased when the humidity in the air passing through the FFR increased for both FFR models.

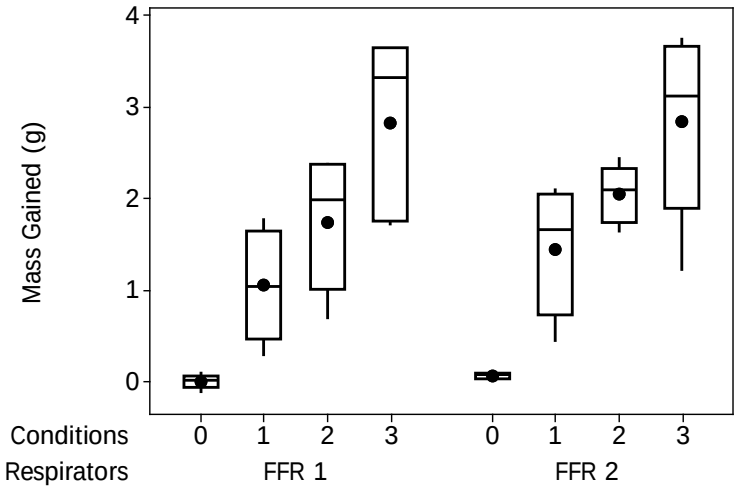

Figure 6. Mass gained for two N95 FFRs (Error bars indicate the range in mass gained).

Filter Layers

The presence or absence of a change in BR generated by air humidity applied to filter layers for each FFR over 30 minutes is summarized in Table V. BR increases were only observed on the middle layer for FFR 1 and on the external layer for FFR 2. WRV magnitude of change is also summarized on Table V. A notable increase in WRV was only observed in the external layer of FFR 1. The magnitude of change in MRV is also summarized in Table V, however, no change was observed on the MRV on the filter layers. Fig. 7 shows SEM micrographs of all the filter layers examined in this study. As can been seen, the inner layer looks similar for both FFR. Similar physical features can also be seen on FFR 1 middle layer and FFR 2 external layer. However, the external layer of FFR 1 is comprised of a different filter media relative to all the other layers; the gaps between the fibers (filter porosity) are greater and fiber diameter is also bigger (Table I).

Table V. Change in breathing resistance (BR), water retention value (WRV), and moisture regain value (MRV) for the individual layers of each FFR.

	FFR 1			FFR 2	
Parameters	Inner layer	Middle layer	External layer	Inner layer	External layer
BR	0.51 ± 0.04	3.63 ± 1.32	0.64 ± 0.05	0.21 ± 0.06	10.4 ± 1.61
WRV	0.030 ± 0.016	0.423 ± 0.037	4.71 ± 0.321	0.013 ± 0.028	0.105 ± 0.007
MRV	0.005 ± 0.002	0.002 ± 0.0003	0.003 ± 0.0003	0.0004 ± 0.001	0.002 ± 0.002

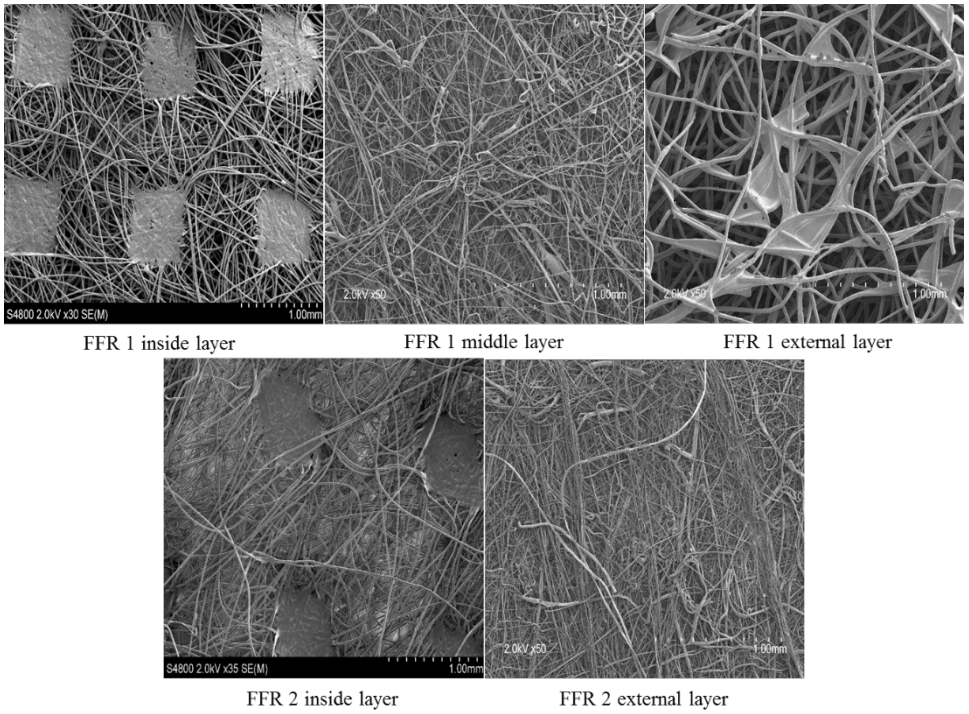

Figure 7. SEM of FFR individual layers (X30-50)

Discussion

This study demonstrated that there was no significant difference in NaCl aerosol penetration after testing the FFRs with simulated air conditions relative to the penetration obtained under typical room air conditions. Our results demonstrate that, even in conditions in which the FFRs gained considerable moisture (Fig. 6), the FFRs retained their particle capture properties. This study also demonstrated that as humidity in air increased, the BR increased after 120 min of testing at simulated heavy breathing and may exceed 20 mm H_2O after 8-hrs. Since no aerosols were used during the BR test described here and distilled water was used to create

the humidity in the air, we can assume that the increase in BR can be related to moisture absorbed within the fibers or adsorbed between fibers of the FFRs.

Previous studies reported an increase or a decrease in particle penetration under humid conditions (Miguel, 2003; Durham and Harrington, 1971). However, those studies both changed humidity levels and challenged the filters with a test aerosol (Al_2O_3 and fly ash) at the same time, so it cannot be determined whether humidity alone affected penetration from those studies. Motyl and Lowkis (2007) demonstrate that humidity will degrade the charge on electret filter media, but that effect required over two weeks of continuous humidity exposure. Gupta et al. (1993) exposed filters to both humidity and a test aerosol and stated that with increasing humidity in air, BR decreased on the filters. Gupta also indicated that these effects are postulated to be due to the filter material type and nature of the particles. Contal et al. (2004) demonstrated an increase in BR through filters when loaded with liquid aerosols for which water may have a similar effect.

Our results also showed a greater increase in BR than reported by Roberge et al. (2010). This increase could be due to a different breathing rate during the cyclic flow and time selected to evaluate the BR. Our study evaluated BR at the worst case scenario, heavy breathing rate, while Roberge (2010) evaluated the BR at a moderate breathing rate (40 L min^{-1}). The difference in breathing rate resulted in a different amount of humid air passing through the FFR and therefore accumulated a greater amount of moisture in the FFRs tested in this study.

As shown in Fig. 6, both FFRs retained moisture compared to the test condition with an increase in MR with increased contact with high humidity air. However, as shown in Fig. 5, when the FFRs were tested in the saturated air conditions the BR outcomes behave differently between the two FFRs. There was an increase in BR for FFR 1 in a range of 1 – 4 mm H_2O for

all three conditions. Whereas BR increased substantially in FFR 2 for Condition 3 with saturated air. An explanation for this effect may be related to the results given in Table V. Those results show that the increase in BR resulting from exposure to humidity occurs primarily in the electret filter media layer (middle for FFR 1 and external for FFR 2). However, FFR 1 has an external support layer consisting of fiber media that resulted in a substantial change in the water retention value (WRV) under high humidity, which may therefore capture moisture before affecting the middle, electret layer. As shown in Fig. 7, the gaps between fibers in the FFR 1 external layer are larger than those in any other layer. Kongdee et al. (2004) provide evidence to show that larger filter gap size, or "pore volume", results in higher water retention between the gaps.

There are several limitations of this work. The Q-Track used to measure relative humidity had a range between 5 to 95%. Our simulated relative humidity was in the upper limit where the Q-Track can measure with reliability. Future studies should use a hygrometer for a more accurate way of measuring the humidity in air. Another limitation was the NaCl aerosol used for the particle penetration test. As relative humidity increases the crystalline NaCl transition to aqueous phase which could affect the particle penetration through the FFR after the BR test. Even though FFRs were sealed and we tested for leakage at high airflow, there may be a possibility that a small leakage would be unnoticed by our testing method. However, we expect the error to be approximately the same for all the tested FFRs.

Despite these limitations our results are still relevant, particularly in determining the importance of testing particle penetration and BR using cyclic flow. Both FFR were N95 certified by NIOSH, however, when tested under cyclic flow and high relative humidity they performed differently. Due to the simulated test conditions used in this study, adding the cyclic flow to the certification protocol could result in an improvement of new FFRs.

Conclusions

Two NIOSH certified N95 FFRs were tested against four different simulated temperature and humid air conditions in a laboratory setting. Results from this study demonstrated that particle penetration was not affected by high humidity. The FFRs, therefore, retained their capabilities as a certified respiratory device when subjected to the tested environmental conditions. Furthermore, high humidity in exhalation air, in inhalation air, or both, increases BR through FFRs. The high porosity external layer of FFR 1 mitigated this effect. Therefore, tasks carried out in high humidity environments may require an evaluation of different FFRs to determine which is less effected by humidity, or reduce the time that an FFR is used by a worker.

CHAPTER III

PARTICLE PENETRATION AND BREATHING RESISTANCE EVALUATION OF UNCERTIFIED DUST MASK

Abstract

The objectives of this study were to determine the maximum particle penetration of uncertified dust masks (UDMs) at the most penetrating particle size (MPPS). An evaluation of the increase in breathing resistance (BR) with particle loading over time was conducted in to compare BR between UDMs and certified filtering face-piece respirators (FFRs). Five different models of commercially available UDMs were selected for this study. Particle penetration of new UDMs were evaluated against a sodium chloride aerosol measured with a scanning mobility particle sizer. Breathing resistance of new UDMs and FFRs were measured for 120 min while challenging the UDMs and FFRs with Arizona road dust for a one-direction airflow at 25°C and 30% relative humidity. Results demonstrated that particle penetration varied by particle size for all UDMs. A wide range of maximum particle penetrations were observed among the UDMs tested in this study (3 – 75% at the most penetrating particle size) ($p < 0.001$). There was a significant difference between the slopes developed between BR and mass loading for the UDMs and FFRs ($p < 0.001$) despite using the same challenge dust. Microscopic analysis of the external layer of each UDMs and FFRs suggests that different collection media in the external layer may influence the particle dust cake developed and therefore affect BR differently between the tested models.

Introduction

Filtering face-piece respirators (FFRs) and uncertified dust masks (UDMs) are filtration devices that remove particles from the air the wearer is breathing (NIOSH, 1995). The National

Institute for Occupational Safety and Health (NIOSH) approves FFRs as a type of personal protective equipment (PPE) to ensure they provide a minimum level of protection against airborne particle exposures in the workplace. The procedures to approve FFRs are provided in the Code of Federal Regulation (42 CFR 84.181) whereas UDMs are not tested against any certification process. However, workers may wear UDMs at some work settings, like agricultural settings, which typically do not fall under Occupational Safety and Health Administration (OSHA) oversight for respirator use.

According to the United State Bureau of Labor Statistics (BLS), an estimated 25 million persons held jobs in agricultural, mines, construction and healthcare settings in June 2015 (BLS, 2015). UDMs are advertised by companies or manufacturers for protection against pollen, dust, diesel fumes, molds, smoke, and other particles and look similar to FFRs. Given the number of workers that are exposed to airborne dust in agricultural, mines, construction and healthcare settings, with similar aerosols as those described for UDM use, it is important to know the performance of UDMs if worn in agricultural, mines, construction and healthcare work settings. Furthermore, with limited published research on UDMs performance, it is unknown how useful UDMs may be to the wearer.

Previous research on UDM performance was conducted to determine filter efficiency, total inward leakage and BR. Cherrie et al. (1987) studied the efficiency of UDMs against cement dust that had a mass median diameter (MMD) of 3 μm. Six subjects wore seven different UDMs and performed a series of tasks simulating light work while wearing the UDMs. Three of the UDMs were cup shaped, two were semi-rigid plastic face pieces, one was a “flat sheet”, and one was a flexible plastic skeleton face-piece. The results indicated that particle penetration ranged between 1.5% - 36%. Wake & Brown (1988) evaluated the filtration efficiency and BR of

UDMs against limestone and cement dust. A test apparatus was used to evaluate 19 UDMs classified into four categories as “cup”, “face pad”, “soft fabric”, and “supported pad”. Initial BR for the UDMs varied from 0.30 mm H_2O to 4.00 mm H_2O. A penetration test was performed at a flow rate of 30 L min^{-1} and at a flow rate equivalent to 150 L min^{-1}. Their results demonstrated that UDMs penetration ranged between 1% and 55% against limestone dust.

These studies suggest that the efficiency of UDMs is not as consistent between models as compared to certified FFRs. For example, all N95 FFRs must have maximum penetrations below 5% for particles in the range 300 nm. However, if a UDM has a higher penetration, it can be expected that it will have a lower initial BR and will be easier to breathe through. Popendorf et al. (1995) found that FFRs were rated worst for “breathing ease” by agricultural workers given a variety of different respirator types. Akbar-Khanzadeh, Bisesi and Rivas (1995) demonstrated that 62% of the workers in a plant that encapsulates automobile glass reported discomfort while wearing half-mask respirators. Meyer et al. (1997) found a significant breathing discomfort during laboratory tests of respiratory protection devices among 30 workers from four factories. Therefore workers may be more likely to use a UDM rather than a certified FFR, which emphasizes the need to evaluate their level of respiratory protection.

Breathing resistance or pressure drop (ΔP) through a fibrous filter at a given airflow results from the restriction to flow caused by both the fabric layer and the particulate layer (Brown, 1989; Novick et al. 1990; Novick, Monson, & Ellison, 1992). Theoretical equations to model ΔP have been studied in the past and are derived from Darcy’s fluid law that states “the variation in ΔP with filtration velocity is constant in the laminar regime” (Letourneau, Mulcey, & Vendel, 1987; Bemer & Calle, 2010). A common expression use to explain the increase in ΔP developed when dust builds on fibrous filters is:

$$\Delta P = K_1 V + K_2 V(M/A) \quad \text{Eq. 8}$$

where K_1 is the filter media resistance (min m^{-1}), V is the filtration velocity (m min^{-1}), K_2 is the particulate layer resistance (min m g^{-1}), M is the mass (g) deposited on the filter media, and A is the filtration media area (m^2) of the filter. When applying Equation 8, the term M / A is often replaced with a term for mass loading (W, g m^{-2}). Previous studies evaluated K_2 for HEPA filters by testing the effect of mass loading on ΔP. Letourneau et al. (1987) and Novick et al. (1992) used three different aerosols with different size distributions as challenge aerosols. Results of their experiments showed that mass loading increases with an increase in particle size. Also, they found that ΔP increases faster with a decrease in particle size. Thomas et al. (2001) studied the influence of various parameters such as air velocity, particle size, and aerosol concentration on ΔP of HEPA filters. Air velocity was tested by using fives different filtration velocities. Results showed that ΔP was higher with an increase in filtration velocities. The effects of particle size on ΔP of HEPA filters was evaluated by using three different particle sizes and two different filtration velocities. Results demonstrated that ΔP is smaller as particle size increases. To test the effects of aerosol concentration on ΔP of HEPA filters, four aerosol concentrations between 5 and 21 mg m^{-3} were used. Results showed that concentrations did not influence ΔP. Currently, most of the published works on ΔP and mass loading have been performed on HEPA filters for enviroment. Knowing if these results can be translated to particle filtering respirator media is important for improving the BR of FFRs .

Previous studies showed that UDMs have limited efficiency. However, new UDM technologies and designs have been developed and are advertised to the public, but their limitations are not well known. As part of this research, we investigated experimentally the maximum particle penetration of a variety of UDMs at the most penetrating particle size

(MPPS). In addition, we evaluated the increase in BR with mass loading over time of unused UDMs and FFRs in an attempt to compare BR between UDMs and FFRs to see if UDMs have a lower BR.

Methods

Respirator Characteristics

Five models of commercially available UDMs and two models of N95 FFRs from different manufacturers were selected for this study (Fig. 8). These UDMs are accessible to the public in retail and online stores. UDM 1 was a three-layer face mask with a rigid external layer followed by a middle layer of electret filter material and a thin inner layer (3M 8661, St. Paul, MN). UDM 2 was a two-layer face mask similar to a multilayer fabric (Breathe Healthy Microbe Shield, Williamsburg, VA). UDM 3 was a two-layer face mask with a removable holder and exhalation valves (I Can Breathe, Chicago, IL). UDM 4 was a one-layer face mask often called a paper mask (MSA 10028549, Cranberry Twp, PA). UDM 5 was a three-layer face mask with a removable holder and exhalation valves (RZ Mask, Chaska, MN.). FFR 1 (3M 8510, St. Paul, MN) was a three-layer respirator with a rigid external layer followed by a middle layer of electret filter material and a thin internal layer. FFR 2 (Moldex 2200, Culver City, CA) was a two-layer respirator with a flexible mesh over the external electret filter material followed by a thin internal layer similar to that of FFR 1. Table VI list the physical characteristics of the tested UDMs and FFRs. The UDMs and FFRs were weighed in a balance with a sensitivity of one mg (Mettler PE 360, Mettler-Toledo LLC, Columbus, OH). The entire thickness of each UDM and FFR was measured using a digital caliper (Neiko 01407A). Scanning electron microscopy (SEM) (Hitachi S-4800, Hitachi High Technologies America, Inc., Schaumburg, IL) of the UDMs and FFRs was

used to analyze fiber diameter. Fiber diameter and surface area were measured using ImageJ software (National Institutes of Health (NIH), Bethesda, MD).

Table VI. UDMs and FFRs Characteristics (Mean ± S. D.)

UDM and FFR models	Number of layers	Mass (g)	Thickness (mm)	Surface area (cm^2)	Fiber diameter (µm)		
					External layer	Middle layer	Internal layer
UDM 1	3	6.46 ± 0.29	0.93 ± 0.05	151.6 ± 1.9	21.8 ± 2.9	7.9 ± 5.2	24.9 ± 5.1
UDM 2	2	16.53 ± 0.65	0.52 ± 0.06	185.6 ± 0.7	14.1 ± 1.3		7.4 ± 1.2
UDM 3[a]	2	12.39 ± 0.58	1.15 ± 0.16	123.6 ± 0.4	15.5 ± 5.2		6.5 ± 0.9
UDM 4	1	3.17 ± 0.14	0.68 ± 0.02	157.3 ± 0.5	7.8 ± 3.9		
UDM 5[a]	3	55.73 ± 0.08	0.88 ± 0.07	177.3 ± 1.1	19.2 ± 2.5	12.5 ± 2.4	5.8 ± 2.2
FFR 1[b]	3	10.48 ± 0.13	1.71 ± 0.09	162.5 ± 1.2	22.1 ± 5.3	5.4 ± 3.2	15.4 ± 1.3
FFR 2[b]	2	14.33 ± 0.54	1.98 ± 0.14	188.2 ± 0.4	5.1 ± 4.6		15.5 ± 1.2

[a] Filter media is contained within additional material

[b] Described on Chapter 2

Figure 8. Images of UDMs and FFRs used in this study

Test System

Two test system were designed to measure UDMs particle penetration and UDMs and FFRs BR with mass loading. Fig.9 shows the experimental setup used for measuring particle penetration and Fig. 10 shows the experimental setup used for measuring BR. A male full round plastic manikin head was used to hold the UDMs and FFRs while performing the particle penetration and BR tests. The manikin head was placed in a 0.055-m^3 acrylic plastic, sealed chamber. As shown in Fig. 9, the manikin head contained a pipe protruding from the mouth area to the back of the head. An additional pipe was used to carry air outside of the chamber. A three-way connector was used to divide the airflow direction, as shown in Fig. 9 and Fig. 10. A pipe connected a vacuum pump to one side of the three-way connector. The available side of the three-way connector was used to insert a tube to the inside of the UDM and FFR for sampling. A second piece of tube was inserted into the chamber and placed beside the manikin head for sampling outside the UDM and FFR. Depending on the test, these two tubes were connected to a three-way valve (Fig. 9) or to the differential pressure sensor (Fig. 10). Air filters were connected to an inlet hole in the side of the chamber to remove particles from the air that entered the chamber.

Penetration Testing

Particle penetration was carried out in the chamber using a NaCl aerosol generated from a 2% solution applied to a nebulizer, as specified by NIOSH to certify N95 FFRs (42 CFR Part 84) modified to not include pre-conditioning the UDMs at 38°C and 85% relative humidity. The environmental conditions during particle penetration test were maintained at 25°C and 30% relative humidity. The aerosol was charge-neutralized with an ^{85}Kr source (Model 3077A, TSI Inc., St. Paul, MN). Fig. 9 shows a schematic of the experimental set-up that was used to measure particle penetration through the UDMs. The generated aerosol was passed through the charge neutralizer, was diluted with filtered air and was sent to the inside of the chamber to generate a steady-state concentration. The aerosol generation was started and allowed to stabilize for five min. A small fan inside the chamber was used to mix the aerosol inside the chamber. The penetration test required continuous airflow at 85 L min^{-1} to be pulled through the filter with a vacuum pump. A flowmeter (Model RMC-104, Dwyer Instrument Inc., Michigan City, IN) and a metered valve were placed between the chamber and the vacuum pump to establish the operational airflow. Airflow calibration was conducted before each test using a calibrator (Model 4046, TSI Inc., Shoreview, MN).

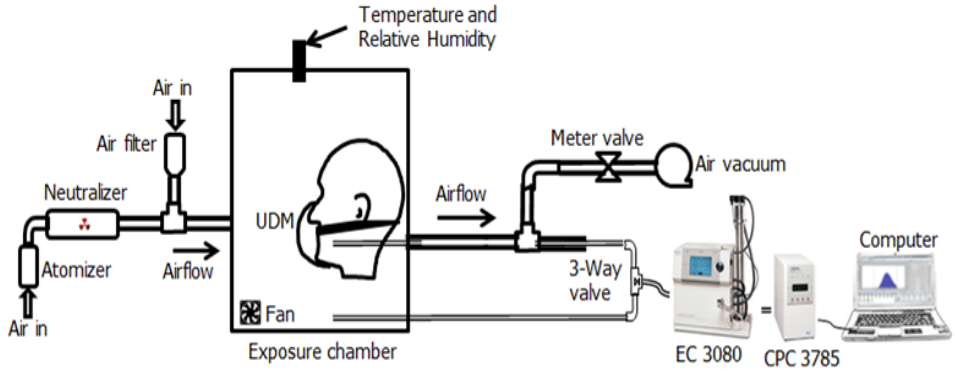

Figure 9. Schematic of the test system used to determine NaCl particle penetration through the UDMs

The particle count and size distribution were measured with a scanning mobility particle sizer (SMPS) consisting of electrostatic classifier (Model 3080, TSI Inc., Shoreview, MN) in combination with a condensation particle counter (CPC) (Model 3785, TSI Inc., Shoreview, MN). The SMPS counted particles within 108 channels ranging between 14–685 nm. As shown in Fig. 9, the sample line to the SMPS was evenly split to enable sampling of particles upstream and downstream the central portion of the UDM. A valve was manually turned to direct flow from one sample line to the other.

During each trial, particle concentration was measured with the SMPS three times in succession outside the UDM, then three times inside the UDM, and then again three times outside the UDM. The particle concentration inside the UDM (C_{in}) was calculated as the average of three measurements inside the UDM and the particle concentration outside the UDM (C_{out}) was the average of the six measurements outside the UDM. The second set of outside measurements ensured that the aerosol concentration remained steady during each test; if the average of the two outside aerosol measurements varied by more than 10%, that trial was rejected and re-conducted (Balazy et al. 2006). The particle penetration, P, was then determined as the ratio of C_{in} to C_{out} for every SMPS size channel:

$$P(\%) = \frac{C_{in}}{C_{out}} \times 100 \qquad \text{Eq. 9}$$

Given the average penetration for all size channels measured during the three trials, the maximum penetration was obtained as well the median diameter of the channel containing the maximum penetration which is the MPPS for the UDMS under the tested conditions.

Breathing Resistance Testing

Inhalation BR was evaluated using mass loading at constant flow. Fig. 10 provides a schematic of the experimental set-up that was used to measure BR through the sealed UDMs and

FFRs. A Wright Dust Feeder was used to introduce Arizona Road Dust (ARD) (Dust Coarse, ISO 12103-1 A4, Powder Technology Inc., Burnsville, MN) inside the chamber (top). A personal DataRam (PDR-1200, Thermo Fisher Scientific Inc., Waltham, MA) was located at the top of the chamber to measure dust concentration inside the chamber of 30 mg m^{-3}. The 30 mg m^{-3} is the double of 15 mg m^{-3} concentration which is the permissible exposure limit for particles not otherwise regulated. The method described by O'Shaughnessy and Raabe (2003) was used to determine the mass median aerodynamic diameter (MMAD) and geometric standard deviation (GSD) of the ARD inside the chamber.

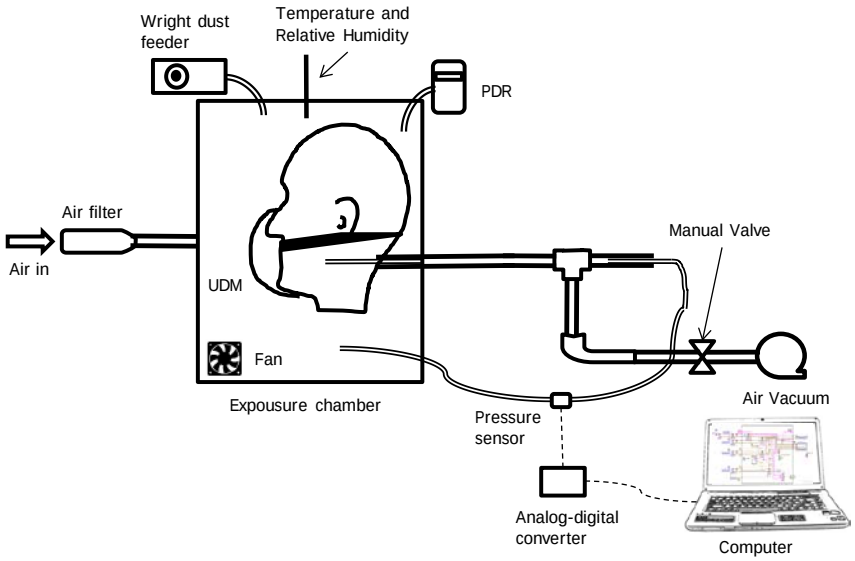

Figure 10. Schematic of the test system used to measure breathing resistance (BR) of the UDMs and FFRs

To simulate inhaled air, a vacuum pump pulled air from outside to the inside of the UDMs and FFRs at 55 L min^{-1}, a flow rate considered to be heavy breathing (Silverman et al. 1951; Stafford et al. 1973). Temperature and relative humidity were maintained at room (23°C, 44%) conditions and were monitored with a factory-calibrated environmental sensor (Q-Trak, TSI, Shoreview, MN).

A calibrated differential pressure sensor (Series 646B, Dwyer Instruments Inc., Michigan City, IN) measured BR across the UDMs and FFRs. As shown in Fig. 10, the pressure sensor was connected with tubing to upstream and downstream UDMs and FFRs. The pressure sensor range was 0-2.5 in H_2O via proportional voltage output of 0.5-4.5 V and was connected to an analog-to-digital converter to measure the voltage with a full scale accuracy of ± 2% (0.05 in H_2O). During each trial, BR measurements were made every 5 s during the 120-min trial period. A one min average over 120-min test was computed. Data were exported to Minitab® (Ver. 17, Minitab Inc., State College, PA) to perform the statistical analyses.

Experimental Design

Tests were conducted to determine the maximum particle penetration of unused UDMs at the most penetrating particle size. In general, the UDMs were sealed to the face of a manikin head with rope caulk pressed firmly to eliminate leakage. To test for possible leakage between the UDM and the manikin face, the BR was measured with a differential pressure sensor while pulling air through at 85 L min^{-1}, and no leakage was assumed if the BR was > 0 mm H_2O. Then, a NaCl aerosol penetration test was performed following NIOSH certification protocol (42 CFR 84.181). The UDMs were preconditioned to laboratory temperature and relative humidity conditions which remained relatively constant near 25°C and 30% relative humidity. A total of five trials per UDM were performed.

A second set of test were conducted to determine dust loading effects on BR of unused UDMs and FFRs for 120-min. For the BR test, UDMs and FFRs were weighed and sealed to the manikin head. Next, ARD generation started and allowed to stabilize and BR test was performed for 120 min. After 120 min, the UDMs and FFRs were removed from the manikin head and

reweighed to determine the mass collected per unit area of the UDMs and FFRs (Eq. 8), or mass loading (W). W was calculated retrospectively using Equation 10:

$$W = VLt \quad \text{Eq. 10}$$

where V is the filtration velocity (m min^{-1}), L is the dust loading (g m^{-3}) and t is the time (min). Then, a regression plot was prepared to compare the change in BR during mass loading for the tested UDMs and FFRs. Regression lines were calculated for each UDM and FFR and the slope of the linear equation divided by V represented the K_2 value (particulate layer resistance). A total of three trials per UDMs and FFRs were performed. UDMs and FFRs were randomly tested.

Quality Factor

The UDMS and FFRs initial quality factor (QF) was calculated to analyze the behavior of an unused UDMS and FFRs as a function of particle penetration (P) and BR. As explained in previous studies (Wake, et al. 1997; Cho, et al. 2011; Huang, et al. 2013) the QF is expressed as:

$$QF(mm^{-1}H_2O) = \frac{ln\left(\frac{1}{P}\right)}{BR} \quad \text{Eq. 11}$$

where P was the mean particle penetration value for an unused UDMs and FFRs and BR was the mean initial BR for an unused UDMs and FFRs. A higher QF represents a better overall performance of the face mask with regards to both penetration and BR at the tested conditions. (Hinds, 1999; Cho, et al. 2011).

Statistical Analysis

Five UDM models and two FFR models were randomly analyzed to assess differences in MPPS, particle penetration, BR, K_2 and QF. All comparisons were conducted as analysis of variance (ANOVA) with statistical significance accepted at $\alpha = 0.05$ level. The mean MPPS value and the mean particle penetration value at the maximum penetration were calculated and analyzed between the UDMs models. Tukey's multiple comparison procedure was used to

determine which UDM model differed in MPPS and particle penetration. The mean initial BR values were calculated and analyzed between UDM and FFR models. The K_2 values were also analyzed between the UDMs and FFRs models. QF values were analyzed using particle penetration and initial BR of the UDMs and FFRs. Data were exported to Minitab® (Ver. 17, Minitab Inc., State College, PA) to perform the statistical analysis.

Results

Particle penetration and MPPS were tested for normality using the Anderson-Darling test and found to be normally distributed. The mean MPPS and maximum particle penetration values for NaCl aerosol (14–685 nm) of the 25 total samples taken for all UDMs are presented in Table VII. Results obtained for two FFRs are also given in Table VII for comparison. The mean BR and K_2 values of the 21 total samples taken for all UDMs and FFRs are also presented in Table VII.

Particle Penetration

The mean MPPS values varied greatly between the tested UDMs and FFRs. The mean MPPS values for the tested UDMs were significantly different ($p < 0.001$). Tukey's multiple comparison procedure showed that MPPS for UDM 1, UDM 3, and UDM 5 were significantly lower than UDM 2 and UDM 4. However, UDM 3 was not significantly different from UDM 4.

Table VII. Mean values of most penetrating particle size (MPPS) and particle penetration of NaCl aerosol (Mean ± S. D.)

UDM and FFR models	MPPS (nm)		Particle Penetration (%)		Initial BR (mm H_2O)		K_2 (min m g^{-1})	QF (mm^{-1} H_2O)
UDM 1	51.3 ± 9.3	C	3.1 ± 1.6	C	10.7 ± 0.2	BC	0.048 ± 0.006	0.33
UDM 2	410.9 ± 124.7	A	74.3 ± 5.9	A	8.1 ± 0.2	D	0.030 ± 0.009	0.04
UDM 3	107.5 ± 16.8	BC	17.2 ± 13.6	C	11.5 ± 0.8	ABC	0.037 ± 0.012	0.15
UDM 4	185.9 ± 39.8	B	47.2 ± 12.1	B	9.8 ± 0.4	CD	0.108 ± 0.010	0.08
UDM 5	58.6 ± 4.2	C	3.5 ± 1.6	C	12.8 ± 1.5	A	0.084 ± 0.029	0.26
FFR 1	41.7 ± 4.7	C	2.8 ± 0.7	C	11.9 ± 0.2	AB	0.021 ± 0.002	0.31
FFR 2	50.5 ± 5.4	C	5.1 ± 1.6	C	13.2 ± 0.4	A	0.108 ± 0.014	0.23

Letters indicates Tukey's analysis

A large range of NaCl particle penetration values were obtained between the UDMs, as shown in Fig. 11. Particle penetration ranged was from 3% to 74 %. The solid vertical line indicates the 5% certification limit established by NIOSH as pass or fail value at the MPPS during the particle penetration test. Mean particle penetration values were significantly different at the MPPS ($p < 0.001$) for each UDM. Tukey's multiple comparison procedure showed that particle penetration for UDM 1, UDM 3, and UDM 5 were significantly lower from UDM 2 and UDM 4.

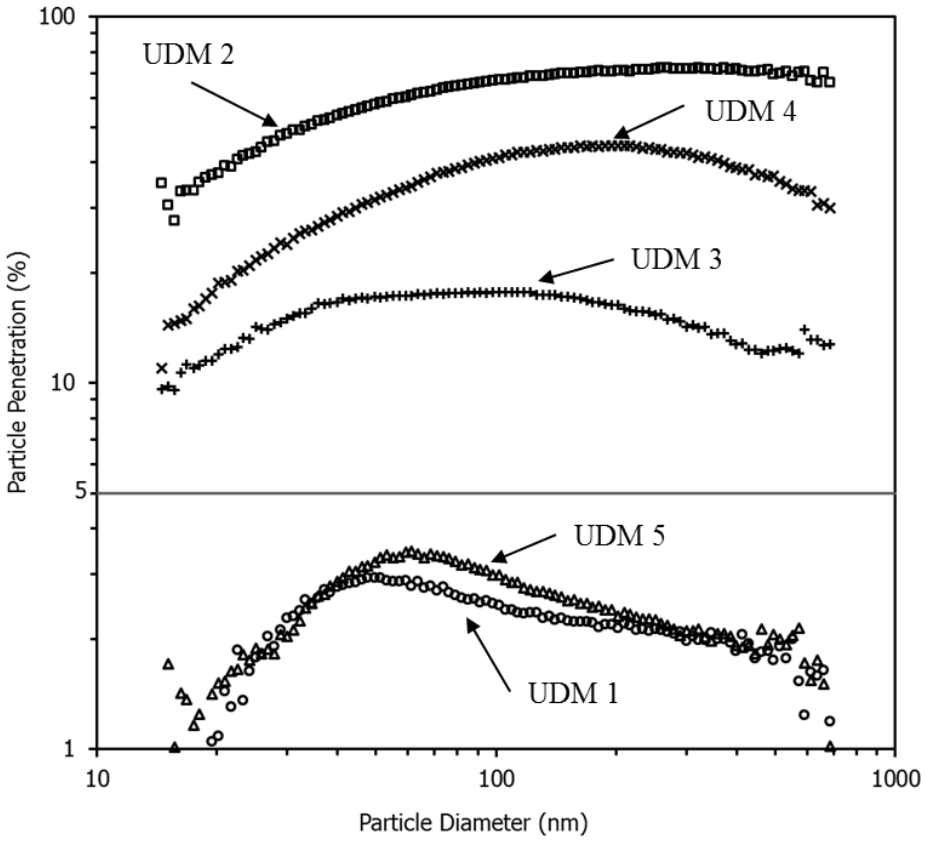

Figure 11. Penetration of NaCl aerosol through UDMs. The solid line represents the 5% certification limit

Breathing Resistance

The calculated mean ARD concentration measured inside the chamber with the direct-reading pDR during the BR test was 26.95 mg m^{-3} (S.D. = 2.82). The measured MMAD for the ARD used was 6.0 µm and the GSD was 3.7 µm.

Table VII shows the mean initial BR values for all the UDMs and FFRs. Table VII also shows the dust layer resistance (K_2) and quality factor (QF) estimates. Differences in the initial BR between UDMs and FFRs were statistically significant ($p < 0.001$). Likewise, the K_2 values differed significantly between the tested UDMs and FFRs ($p < 0.001$).

The slopes developed from the linear association between BR and mass loading (W) for all UDMs and FFRs are shown in Fig. 12. As can be seen in that figure, the net increase in BR ($\Delta P - \Delta P_0$) was plotted as a function of W to emphasize the differences in the observed slopes. Based on Eq.10, the slopes in Fig. 12 divided by filtration velocity represents the K_2 value for each UDM and FFR when loaded with ARD. The slopes relating an increase in BR as W increased were different between all the tested UDMs and FFRs ($p < 0.001$).

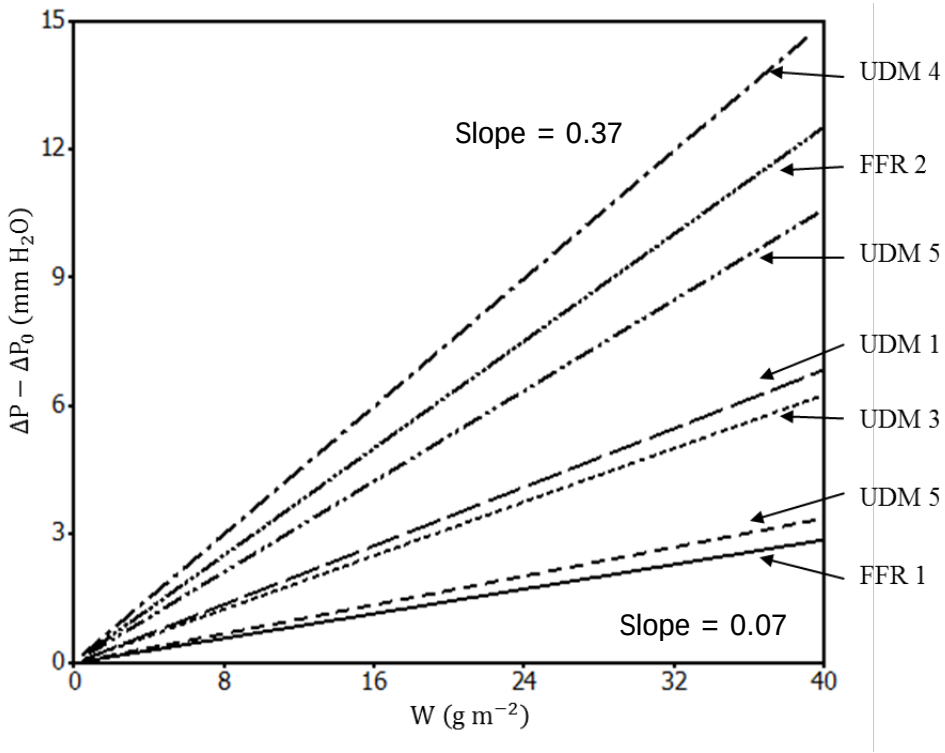

Figure 12. Net BR as a function of mass loading for different UDMs and FFRs

Fig. 13 shows SEM images of the UDMs and FFRs' external layer loaded with ARD at the end of the 120-min trial. Differences in dust cake formation can be seen across UDMs and FFRs depending on the composition of the UDMs and FFRs' external layer. For example, UDM 4 and FFR 2 show a very dense dust layer on external of small-diameter fibers that may contribute to the high K_2 values determined for those UDMs and FFRs. Conversely, FFR 1 and UDM 2 have low K_2 values.

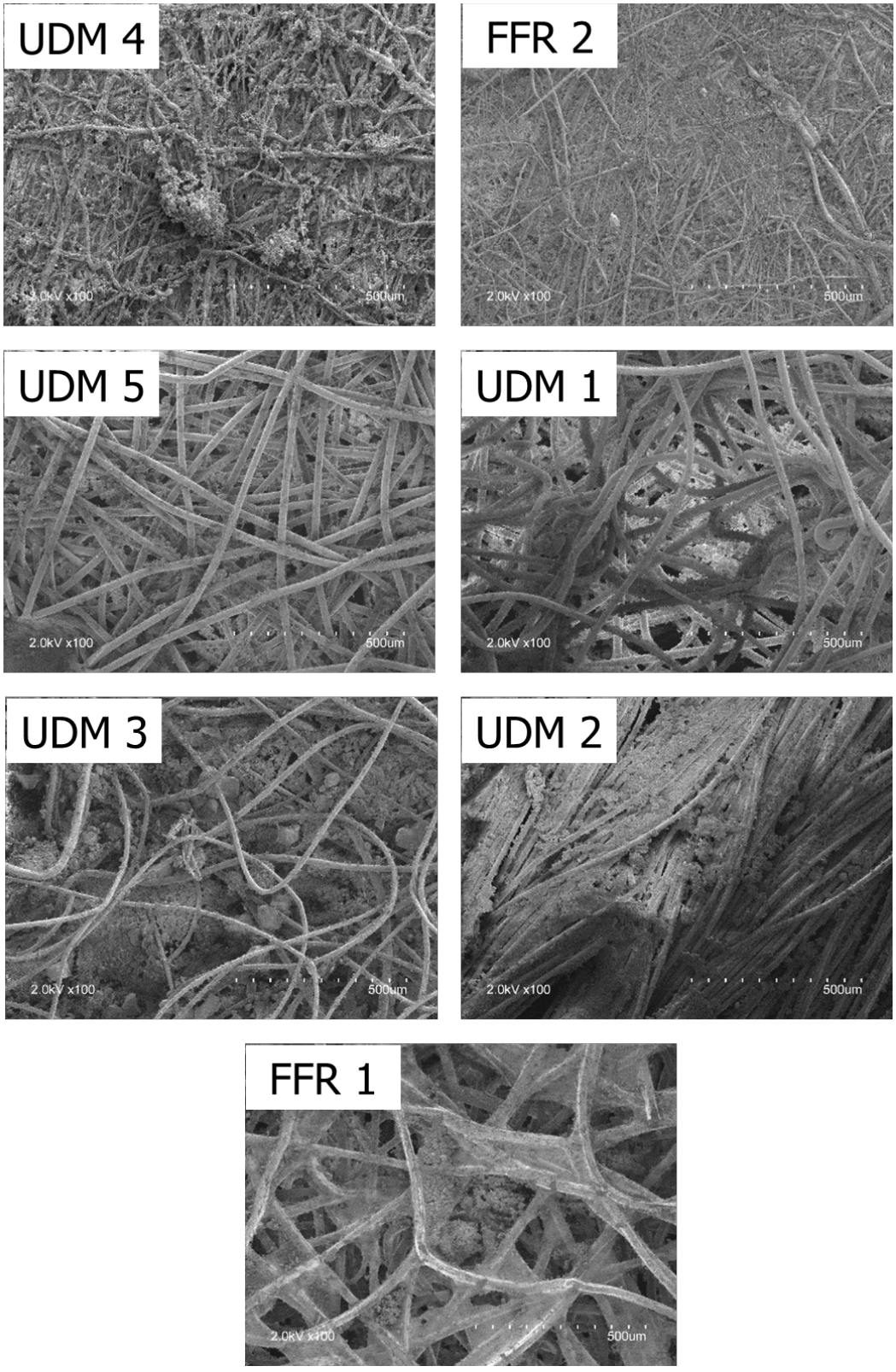

Figure 13. SEM images of external layer of loaded UDMs and FFRs with ARD (X100) (presented in order of Fig. 12)

The QF values shown in Table VII differed significantly between the tested devices ($p < 0.001$). FFR 1 and UDM 1 resulted the higher QF with values of 0.31 and 0.33 mm^{-1} H_2O respectively. UDM 2 and UDM 4 resulted with the lowest QF with values of 0.04 and 0.08 mm^{-1} H_2O respectively.

Discussion

The results in this study demonstrate that unused UDMs had a particle penetration that varied greatly against NaCl aerosol. Particle penetration for three of the UDMs exceeded the 5% particle penetration that NIOSH use as the maximum allowed value for certifying FFRs (NIOSH, 1995). The variation in particle penetration in UDMs obtained in this study coincide with results previously reported (Cherrie et al. 1987; Wake & Brown, 1988; Rengasamy, Eimer, & Shaffer, 2010).

Particle penetration of NaCl aerosol in the range of 10-700 nm measured in five different UDMs models showed a broad range in MPPS. Observed MPPS greater than 100 nm was associated with filters that do not have electrostatic fibers in their filtering media (Fardi, 1991; Balazy, et al. 2006; Eshbaugh, et al. 2009; Rengasamy, BerryAnn, & Szalajda, 2013). Also, MPPS lower than 100 nm was associated with filters that are composed of electrostatic fibers in their filtering media. The results obtained in this study suggest that some UDMs incorporated electrostatic fibers in their filtering media while others do not. Having the electrostatic fibers in filtering media allows for multiple types of capture mechanisms acting in the filter media based on particle size.

Our study suggests a decreasing tendency in particle penetration in four out of the five UDMs tested against particle size greater than 200 nm. The decrease in particle penetration for particles greater than 200 nm indicates that users may benefit from using UDMs during work in

industries where workers are exposed to aerosols greater than 100 nm. However, even though face seal leakage was not tested in this study, previous studies demonstrated high particle penetration through the edges of unfitted UDMs (Guyton, et al. 1956; Cherrie, et al. 1987). Future UDMs studies should include an evaluation of face seal leakage during particle penetration tests of UDMs designs.

The present study demonstrated differences in initial BR between UDMs and FFRs. As expected, UDMs had an initial BR lower than FFRs. However, that difference was not as high as expected considering that UDM 2, UDM 3 and UDM 4 had the highest particle penetration. However, the electrostatic fibers on FFRs used to provide a lower particle penetration without increasing BR may be the reason that the difference between BR was not as large as expected among the tested UDMs and FFRs.

Differences in BR were observed between UDMs and FFRs with ARD mass loading. Theoretically, when the same dust is applied to any filter media, the increase in BR associated with W should be similar. In other words, the K_2 value should only be dependent on dust properties and not vary by filter media type as shown in Fig. 12. The observed variability in K_2 may be explained by the difference in the dust layer formed on the surface of the UDMs and FFRs. Barret & Rousseau (1998) demonstrated how the dust layer formed at a different rate depending on filter fibers properties. Cho et al. (2011) also observed an increase in BR when respirators were loaded with welding fume. Results from this study suggest that these differences in K_2 can be related to different filter fiber diameter and thickness especially in the external filter layer of the UDMs and FFRs.

SEM images taken of the UDMs and FFRs surface after they were loaded explain how dust layer deposited on each UDM and FFR. As those illustrations show, particle deposition is

scattered across the external layer of some UDMs and FFRs, while in other UDMs and FFRs particles are more densely deposited on the external layer. Cho et al. (2011) showed differences in dust layer formation on FFRs when loaded welding fumes on the SEM images. When the external layer is composed of thick fibers instead of thin fibers, the external layer with thick fibers prevented the formation of the dust layer. SEM image of FFR 1 shows the thick fibers of the external where particles are deposited but there is no dust layer formation. In comparison, FFR 2, with thinner fibers on the external layer clearly shows the dust layer formation. The differences in K_2 values between the FFRs may be explained by the larger-diameter fibers in FFR 1 creating larger gaps to minimize resistance in air flow through the FFRs.

The QF associates particle penetration and BR to obtain a qualifying value to rate respirator performance, based on Eq. 11. Low particle penetration and BR represents the highest QF. FFRs and some UDMs would have a low penetration and corresponding high BR, while the penetration measured for the other UDMs would be high but with an offsetting low BR resulting in comparable QF values between the two groups. However, UDM 2 had a 70% particle penetration, higher among the tested UDMs and FFRs, but the initial BR value of 8 mm H_2O was not low enough to offset the high particle penetration result and obtain a QF value comparable to the FFRs tested. UDM 3 and UDM 4 showed a similar effect but to a lesser extent. For UDM 2, UDM 3 and UDM 4 to obtain a QF similar to FFR 1, a very low BR (1-6 mm H_2O) would be needed to compensate for the high particle penetration. Therefore, our results indicate that the lower performance by some UDMs in terms of high particle penetration is not offset by a significant decrease in BR.

UDMs have been advertised for worker protection as protective and comfortable alternatives to available FFRs. UDM 2, UDM 3, and UDM 5 are non-traditional style, with

different shape than a N95 FFR. Despite being the least efficient in particle penetration in the range of 10-700 nm, UDM 2 may be the most comfortable because of the soft material used in the inside layer. UDM 3 and UDM 5 have a similar style of filter media separated from the mask and exhalation valves. The reason for having the filter media separated from the mask is to allow for the filtration media to be replaced. As shown in Table VI, the mass of UDM 3 (12.4 g) is different from the mass of UDM 5 (55.7 g). The difference in mass between UDMs may affects how preferable the UDM may be, after wearing the UDM for a period of time. Moreover, the exhalation valves in UDM 3 and UDM 5 were difficult to replace.

There are several limitations of this work. Leakage between the mask and manikin may have occurred and was not evaluated in this study. However, after every experimental trail, the seal between the mask and manikin was examined and no seal failure was observed. Only a limited number of UDMs and FFRs models were tested in this study. Others UDMs and FFRs models may perform differently. Cost and worker comfort of UDMs and FFRs were not evaluated. Future research should study UDM and FFR cost, worker comfort, particle penetration and BR.

Conclusions

Five UDMs were tested against NaCl aerosol in a laboratory setting to evaluate particle penetration through these UDMs. Results from this study demonstrated a wide range in particle penetration against NaCl aerosol among UDMs. Aerosol penetration among three of the UDMs were above the 5% minimum level recommended by NIOSH at the MPPS.

The increase in BR with mass loading of five UDMs and two NIOSH certified N95 FFRs were experimentally tested in this study. Results demonstrated that the increase in BR with mass loading was different between the tested UDMs and FFRs. Differences in the structures of the

external layer may influence particle deposition and affect BR differently between the tested models.

We did not observe a significant reduction in BR to compensate for the high particle penetration of some UDMs. Therefore, assuming BR is an important criteria for face mask use by workers in the agricultural sector, then the UDMs did not have the expected low BR relative to a high penetration that would justify their use by those workers.

CHAPTER IV

BREATHING RESISTANCE EVALUATION THROUGH FILTERING FACE-PIECE RESPIRATORS WORN DURING THE POWER WASHING TASK IN SWINE BUILDINGS

Abstract

The objective of this study was to determine the breathing resistance (BR) of filtering face-piece respirators (FFRs) while performing power washing in a swine building. Two models of commercially available N95 FFRs, referred to as FFR 1 and FFR 2, were selected for this study. BR of new FFRs were measured for 120 min while a member of the research team wore the FFR while performing power washing during winter in multiple swine rooms. Temperature and relative humidity were recorded during the power washing tasks. Results demonstrated that BR of the tested FFRs did not increase during power washing in a Control Room (FFR 1, $p = 0.40$; FFR 2, $p = 0.86$). Workers wearing a new FFR while performing power washing in swine rooms should not detect any difference in BR, at least for 120 min of power washing. Based on this study, FFR wearer should expect no increase in BR over 8 hr of power washing, decrease health risk by wearing the FFR and no need to replace the FFR during the power washing task.

Introduction

Animal Feeding Operations (AFO) are agricultural operations where animals are kept and raised in confined situations. AFOs concentrate animals, animals' feed, manure and urine, dead animals, and production operations within a small area of land. Swine farms are an example of an AFO where swine are held and grown for up to 45 days for meat production and animal breeding. Sixteen percent of swine farms in the United States each produce 1,000 or more swine per year (USDA, 2014). The increase in building size to accommodate more swine and fulfill the consumer demands may increase the workers' exposure to dust generated inside the building.

The organic dust found in swine buildings commonly contains biologically active materials like microbes, endotoxins and pathogens (bacteria and viruses) that can lead to pulmonary symptoms such as congestion, coughing or wheezing, and sensitivity to dust (Gustafsson, 1997). Moreover, an increased frequency of infections including colds, bronchitis, and pneumonia have been reported among workers exposed to organic dust (OSHA, 2009). Dust concentration inside swine buildings have been study in the past. Donham et al. (1989) measured 'total' dust concentration using personal samplers in 30 swine buildings and reported a mean 'total' dust concentration of 6.8 mg m^{-3}. Donham et al. (1995) measured 'total' dust concentration on 108 swine farmers during the spring, autumn and winter seasons and demonstrated that workers were exposed on average to 4.53 mg m^{-3}. Larsson et al. (2002) measured a mean inhalable dust concentration of 0.94 mg m^{-3} and a mean respirable dust concentration of 0.56 mg m^{-3} among sixteen subjects while power washing swine rooms. O'Shaughnessy et al. (2012) measured a mean of 40,300 endotoxin units m^{-3} endotoxin concentration of personal sampling while power washing swine rooms.

Previous studies have documented adverse respiratory health effects of workers exposed to organic dust in indoor swine buildings. Larsson et al. (1994) exposed fourteen healthy subjects to swine dust for 2 – 5 hours of work and demonstrated that the swine dust exposure increased the number of alveolar macrophages, neutrophils, eosinophils, and lymphocytes in the bronchoalveolar lavage in healthy subjects. Wang et al. (1997) exposed twenty-two healthy subjects to swine dust ('total' concentration range was 14.6-30 mg m^{-3}) for three hours and observed that subjects experienced symptoms of shivering, headache, malaise, and muscle pain. Moreover, granulocytes, lymphocytes, and monocytes in the bronchoalveolar lavage and total cells in nasal lavage increased in all subject after being exposed to the swine dust.

Dosman et al. (2000) studied the effectiveness of using N-95 disposable respirators as an intervention in swine barns on twenty-one healthy subjects for 4 hours of work. Subjects self-reported, on average, more cough, chest tightness, and phlegm symptoms on the days where no intervention was used. Additionally, the mean total number of cells measured in the nasal lavage was higher on nonintervention days. Zedja et al. (1993) performed a cross-sectional survey among swine producers and identified that workers who used a dust masks had fewer respiratory symptoms of chronic phlegm, chest wheezing, and better lung function than producers who did not use the dust mask. Larson et al. (2002) studied the health effects of human subjects exposed to dust generated during power washing among sixteen swine workers, where seven subjects used a respirator during the power washing. They identified that the aerosolized material (dust) generated by power washing was associated with an increased number of inflammatory cells in the upper respiratory airways in subjects not wearing a respirator compared to subjects wearing a respirator. These studies suggest that swine farm workers who are exposed to organic dust often experience adverse respiratory health effects. Minimizing workers' exposure to dust should be a priority for reducing health-effects of workers in swine buildings.

General ventilation is an approach used to control dust particles in swine buildings. Dust particles inside these buildings are generated from multiple sources, including feed particles, skin dander, and dried fecal material (Donham et al. 1986). However, current ventilation design parameters in swine buildings are based on the removal of moisture and heat generated by the animals, not on the mitigation of dust (O'Shaughnessy et al. 2010). Few studies have implemented engineering controls as a dust reduction method. Nonnenmann et al. (2004) implemented oil sprinkling to reduce dust concentration inside swine production buildings and their results showed that the use of the oil sprinkling system reduced average 'total' dust

concentration by 52% (from 1.39 to 0.65 mg m^{-3}). Anthony et al. (2014) modeled the effectiveness of five air pollution control devices (shaker dust control, electrostatic precipitator, cyclone wet dust collector and trickle filter) in a small farrowing barn. All devices reduced inhalable dust concentration below the 2.8 mg m^{-3} exposure recommended for industry. Anthony et al. (2015) evaluated the effectiveness of a shaker-dust collector in reducing dust concentrations in recirculating air. Inhalable dust concentration was reduced 33% (from 1.01 mg m^{-3} to 0.68 mg m^{-3}) and respirable dust concentration was reduced 41% (from 0.20 mg m^{-3} to 0.12 mg m^{-3}). Even though, there have been recent improvement of general ventilation in animal indoor facilities, filtering face-piece respirators (FFR) still are a suitable personal protective equipment (PPE) used to reduce worker exposure to dust because of their cost and accessibility.

The National Institute for Occupational Safety and Health (NIOSH) certifies FFRs to ensure they provide a minimum level of protection against airborne particles in the workplace. The performance conditions used by NIOSH to certify FFRs are explained in the Code of Federal Regulations (42 CFR 84.181). One of the evaluation criterion for certifying FFRs is breathing resistance (BR). BR is used to evaluate how difficult it is for the wearer to breathe when wearing the FFR, the higher the BR the harder it is to breathe. When the wearer notices increased BR, they should change the FFR for a new one. The Survey of Respirator Use and Practices (BLS, 2002) gathered information on respirator use in the Agriculture, forestry, and fishing industry. The survey showed that of the 13,200 establishments surveyed only 3,300 (5.8%) employees reported using any respirators. Also, of those 13,200 establishments, 10,600 (80.3%) reported using disposable dust masks. Mitchell & Schenker surveyed 588 Californian farmers from 1993 to 2004 to determine if Californian farmers changed their respiratory

protective behavior and their results show that use of dust mask or respirator decreased from 45% (267 farmers) in 1993 to 33% (194 farmers) in 2004. The limited use of respirators in agricultural industry are associated to the willingness of the worker to wear the respirator, and to comfort and inability issues when wearing the respirator, like BR (Graveling et al. 2010; Mitchell & Schenker, 2008; Doney et al. 2005; Popendorf et al. 1995).

The purpose of this study was to evaluate changes in the BR of two models of N95 FFRs while performing power washing in indoor swine production. This study also characterized the environmental conditions (temperature and relative humidity) during the task of power washing. The results of this study are anticipated to increase the understanding of how field conditions affect the BR of FFRs and to identify whether the increased BR thru FFRs is a plausible barrier to adopting their use in the swine industry.

Methods

Filtering Face-piece Respirators (FFRs)

Two models of N95 FFRs from two manufacturers were used in this study and will henceforth be referred to as FFR 1 and FFR 2. Both FFR 1 and FFR 2 are used in occupational settings and have different physical characteristics that could effect their performance in varying environmental conditions. FFR 1 (3M 8510, St. Paul, MN) is a three-layer mask with a rigid external layer, a middle layer of electret filter material, and a thin inner layer. FFR 2 (Moldex 2200, Culver City, CA) is a two-layer mask with a flexible mesh on the outside of an electret filter material and a thin inner layer similar to that of FFR 1. Physical characteristics of the tested FFRs were described in Chapter 2. Fig. 14 shows the images of the tested FFRs.

Figure 14. Image of FFRs used in this study

Site Description

Two swine facilities located in east Iowa, an education center and a family-owned facility, were visited during the winter seasons of 2013-14 and 2014-2015. The first facility, Mansfield Swine Education Center located in Cedar Rapids, IA, consisted of farrowing, finishing and nursery buildings. The farrowing building consisted of three different rooms connected by an internal hallway. The finishing building consists of six similar rooms connected by an outside corridor. The second facility, a family-owned swine farm located in Davenport, IA, consisted of farrowing-nursery and finishing buildings. The farrowing room was connected to the nursery room in the same building. Only the farrowing room was power washed in this study.

Power washing was performed in clean and dirty rooms. A clean finishing room, identified as Control Room, was used to observe the effects of power washing on FFRs BR between models. Three trials were performed in the Control Room. Then, power washing was performed on dirty finishing rooms, identified as Test Room #1, and dirty farrowing rooms, identified as Test Room #2. Two trials were performed in Test Room #1 and four trials were performed on Test Room #2.

Physical characteristics were recorded for the power washed rooms in each building (Table IX). Two finishing rooms in the Education Center were used as a Control Room and Test Room #1. Fig. 15 shows an image of the Test Room #1. Fig. 16 shows an image of Test Room #2.

Table VIII. Characteristics of swine rooms that were power washed

Rooms characteristics	Control Room & Test Room #1	Test Room #2	
		Farrowing room at Education center	Farrowing room at family-owned
Type	Room with side curtains	Closed room	Closed room
Flooring	Concrete slotted	Plastic slotted, concrete hallway	Plastic slotted, concrete hallway
Room dimensions (L x W, ft)	34 x 28	50 x 28	40 x 40
Room capacity	50 – 80 swine	19 sow crates	28 sow crates
Pit (deep, ft)	4	4	8

Figure 15. Test Room #1 at Mansfield Swine Educational Center

Figure 16. Test Room #2 at Mansfield Swine Educational Center

A further description of the swine rooms where power washing was performed is given. Fig. 17 shows the distribution of air for Control Room and Test Room #1. Air entered the building through roof baffles and was mixed in the attic. Celling inlets allowed air to move from the attic to the room in the building being power washed. A pit fan removed air from the room through the slotted floor to the pit and to the outside of the room. The pit fan and ceiling inlets were controlled by thermal sensors located inside the room and connected to a control panel inside room. The Control Room and Test Room #1 have two square ceiling inlets located to the sides of the room. The heater was on while power washing, however, because no animals were inside the room operating conditions were kept to minimum.

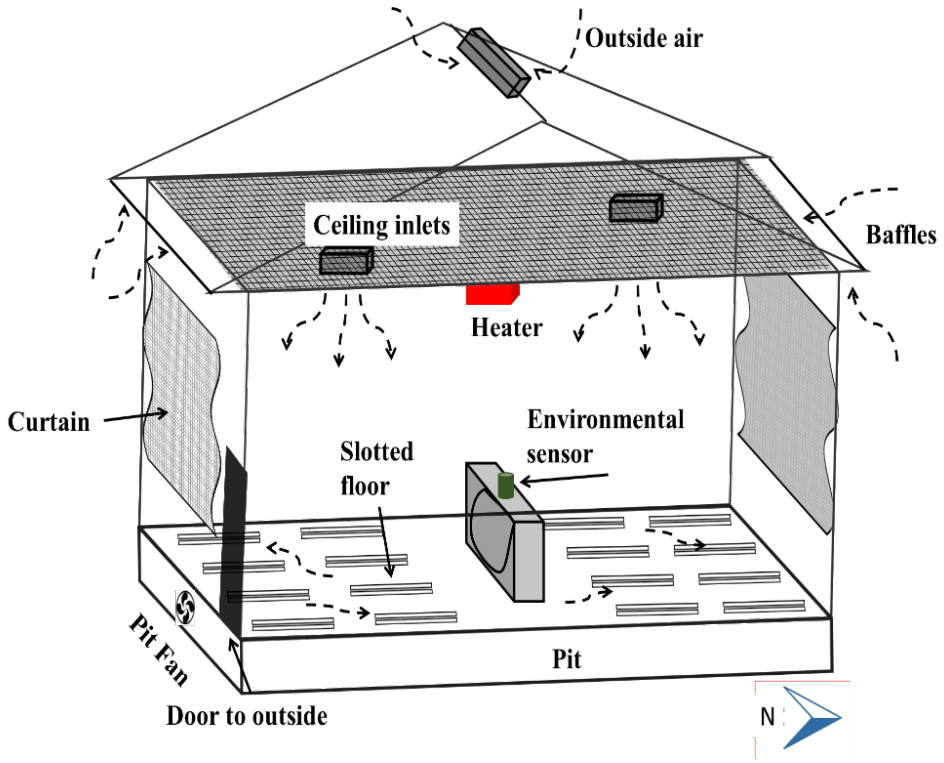

Figure 17. Schematic diagram of Control Room and Test Room #1

Fig. 18 show the distribution of air process for Test Room #2. As can be seen, air entered Test Room #2 similarly to the Control Room and Test Room #1. Differences were observed in the pit fans and ceiling inlets locations. The pit fans in Fig. 17 were located to the south of the room while pit fans in Test Room #2 (Fig. 18) were located to the west side of the room. The ceiling inlets in Test Room #2 were located in the center of the room from the west side to the middle of the room. Another detail is the two baffles on the east side of Test Room #2 (Fig. 18). The east side of Test Room #2 is connected to a hallway and two other rooms. Warm air was also drawn from the hallway through those baffles in Test Room #2 when the pit fans were in operation. Fans located on the north and south walls of Test Room #2 were sealed during the winter season.

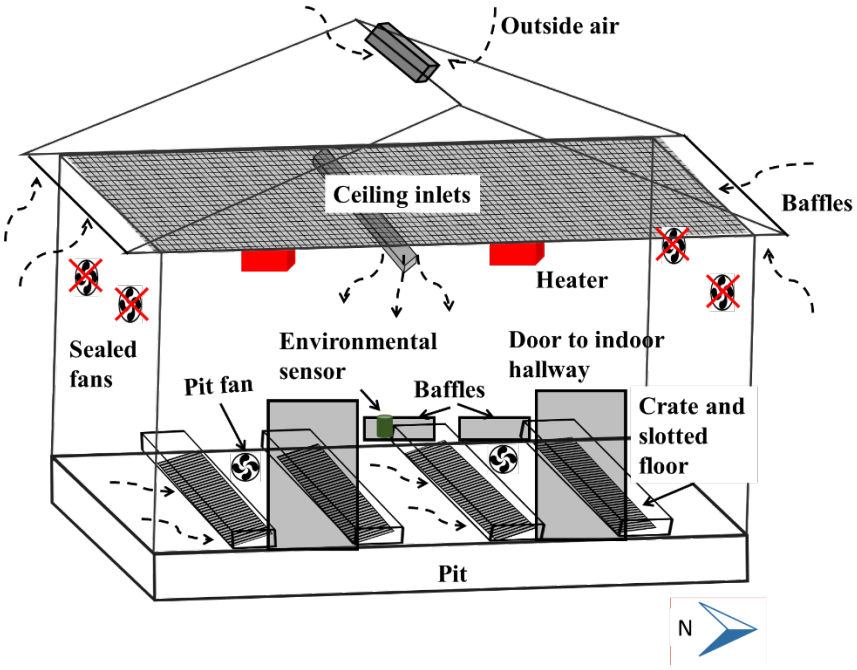

Figure 18. Schematic diagram of the Test Room #2

Power Washing

Power washing was performed by a member of the research team after receiving instruction from the administrator of both facilities. Power washing began end of the room and moved to the other end while spraying in the direction of movement. Floor, cages, feeders, walls (from the floor to half way up the ceilings) within the room were washed thoroughly. The nozzle of the power washer was maintained between 15-30 cm from the surfaces cleaned. Table IX shows the properties of the available power washers used in this project.

Table IX. Properties of the power washers (PW) used

PW Equipment	Mansfield Swine Education Center	Family owned swine farm
Type	Electric	Gas
Engine Horsepower	7.5	12
RPM	1450	3600
Pressure (PSI)	3500	2000
Water Flow Rate ($cm^3\ s^{-1}$)	315.5	252.4
Nozzle Type	Round	Round
Cold or Hot Water	Cold	Cold

Test System

A test system was designed to measure the inhalation BR of FFRs while performing power washing in swine buildings. The FFR BR was measured by sealing the outer edge of the FFR that typically seals against the wearer's face between two acrylic plates. The two plates were held together with screws in each corner that was tightened to ensure there was no air leakage between the FFR and the acrylic plates. The acrylic plates were attached to a threaded pipe that was connected to a three-way connector as shown in Figure 19. Another side of the three-way connector was connected to a vacuum pump (Model 5KH36KN90HX, Fisher Pump, Pittsburgh, PA). The other side was used to insert a tube downstream of the FFR and connect to a differential pressure gage (Series 2000, 0–75 mm H_2O, Magnehelic, Dwyer Instruments, Michigan City, IN), as shown in Fig. 19.

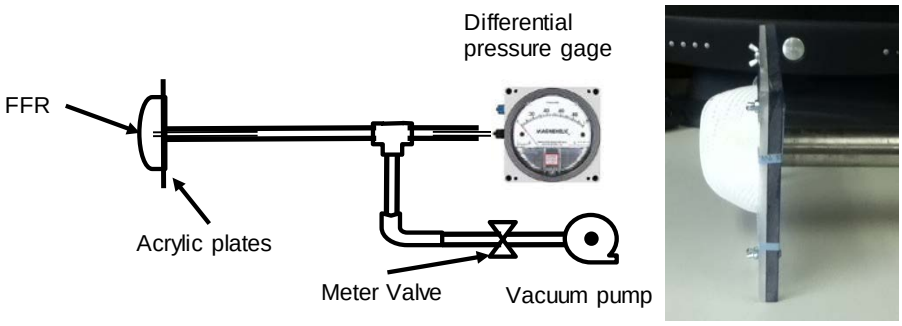

Figure 19. Schematic of the system used to measure BR at swine rooms and the FFR sealed between the acrylic plates

Sampling Methods

FFR mass was measured in a balance with a sensitivity of five mg (Model i101, 100 g, MyWeight, Phoenix, AZ) before power washing started. Then, an initial BR measurement was taken by sealing the FFR between the acrylic plates. BR was measured under simulated heavy inhalation air with the vacuum pump pulling air from upstream to downstream of the FFR at 55 L min^{-1}. Flow rate was maintained with a meter valve and measured with a flowmeter (Series RMA, Dwyer Instruments, Michigan City, IN). The differential pressure gage was used to

measure BR across the FFR and the BR value was recorded. Then, the FFR was removed from the acrylic plates, donned by the researcher and the researcher began to power wash the swine room. The researcher stopped power washing every 30 min, removed the FFR, and BR was measured using the setup in Fig. 19. Once the researcher washed half of the room, the FFR was removed, BR was measured and the FFR mass was recorded. The researcher switched for the other FFR model. Initial mass and BR was measured for the second FFR model and the same researcher started to power wash the other half of the room. Again, BR was measured every 30 min until the power washing was complete when final BR and FFR mass was obtained for the second FFR model. FFRs were randomly tested during the same day.

Temperature and relative humidity measurements were taken throughout the power washing process using a factory calibrated environmental sensor (Q-Trak, TSI, Shoreview, MN). For the Control Room and Test Room #1, temperature and relative humidity were measured in the center of the room three ft above the floor. For Test Room #2, temperature and relative humidity were measured in the center of the room three ft above the floor or next to the baffle five ft above the floor.

Statistical Analysis

Breathing resistance data was assessed for each FFR model per power washed swine room. Linear regression was used to identified the slope and intercept between BR and time of wearing FFR during power washing. Recorded data of pre- and post- FFR mass was also analyzed. Descriptive statistics (mean and standard deviation [SD]) was generated for each FFR model per power washed swine room. A two-sample T-tests was conducted to compare the mass gained between FFR models. Data from Q-track was processed by power washing task.

Descriptive statistic for temperature and relative humidity (mean and standard deviation [SD]) were generated per swine room. A statistical significance was accepted at the α=0.05 level.

Results

Temperature and Relative Humidity

Temperature and relative humidity varied over the power washing task. The mean temperature and relative humidity during power washing by room are shown in Table XI. Figure 20 show an example of the the temperature and relative humidity during the power washing task on Test Room #1. Temperature outside the Test Room #1 was near 1°C (34°F) and 60% relative humidity before starting power washing. Inside Test Room #1, temperature was 7°C (45°F) and 70% relative humidity. During power washing, temperatures ranged between 7°C to 13°C (45°F – 55°F). Relative humidity ranged between 80% to 100%. The heater inside these rooms were kept in minimal operation. Similar temperature and relative humidity values were measured inside the Control Room. As shown in Fig. 20, relative humidity peaks represent every time power washing stopped to measure BR of the FFR being tested.

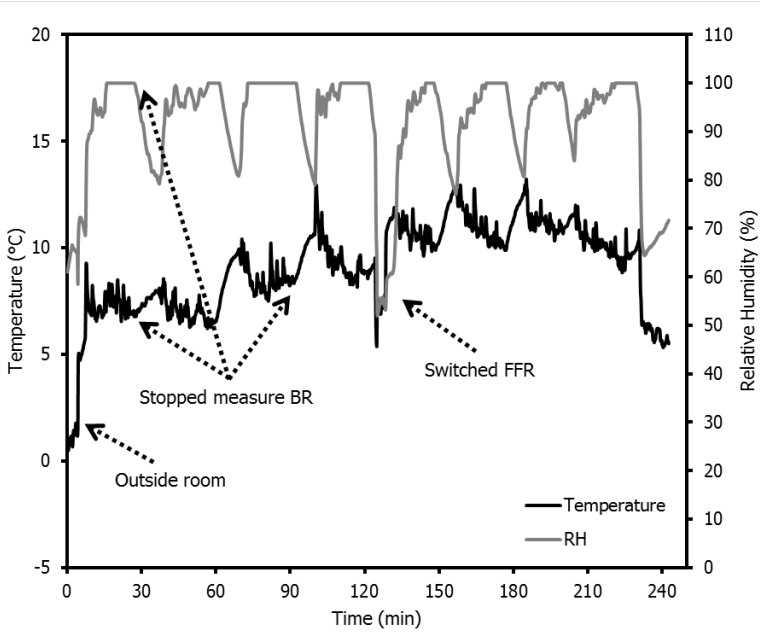

Figure 20. An example of temperature and relative humidity during power washing Test Room #1

Figure 21 show an example of the temperature and relative humidity during the power washing task on Test Room #2. Temperature in Test Room #2 was higher than Test Room #1 and ranged between 15°C (59°F) to 19°C (67°F). Also, changes in temperature were less frequent in Test Room #2 than in Test Room #1. Relative humidity ranged between 80% and 100%, however, it took more time to reach 100% than in Test Room #1. Also, relative humidity it did not stay at 100% during the power washing task. In addition, there is a temperature peak that could indicate that the heater or pit fan began to operate as there was an increase in temperature and a decrease in relative humidity, as shown in Fig. 21.

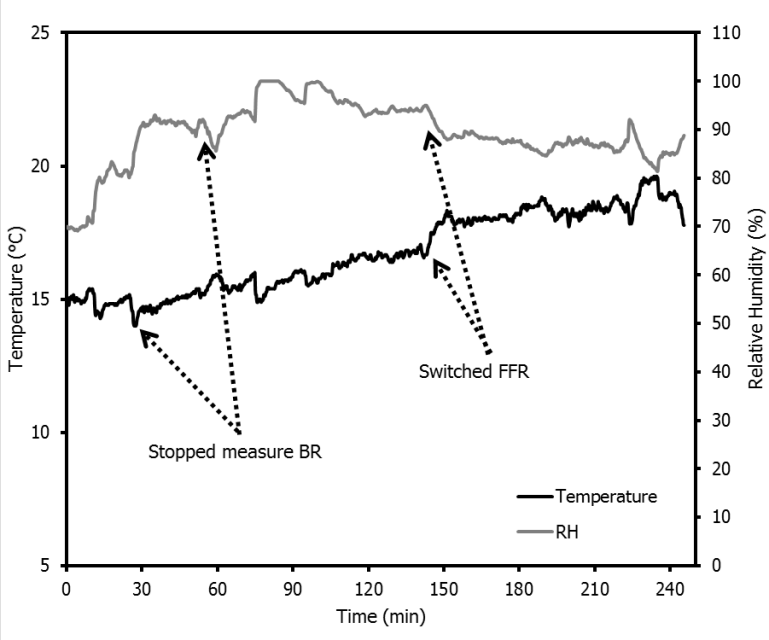

Figure 21. An example of temperature and relative humidity during power washing Test Room #2

Breathing Resistance

The BR of two FFRs was evaluated during the power washing of swine rooms performed during the winter season. A total of nine days were sampled during the two winter periods. The measured BR of FFR 1 and FFR 2 while power washing the Control Rooms is shown in Fig. 22. A linear relationship between time and BR demonstrated that no increase in BR was observed between the tested FFRs during the 120 min power washing tasks (FFR 1, $p = 0.40$; FFR 2, $p = 0.85$).

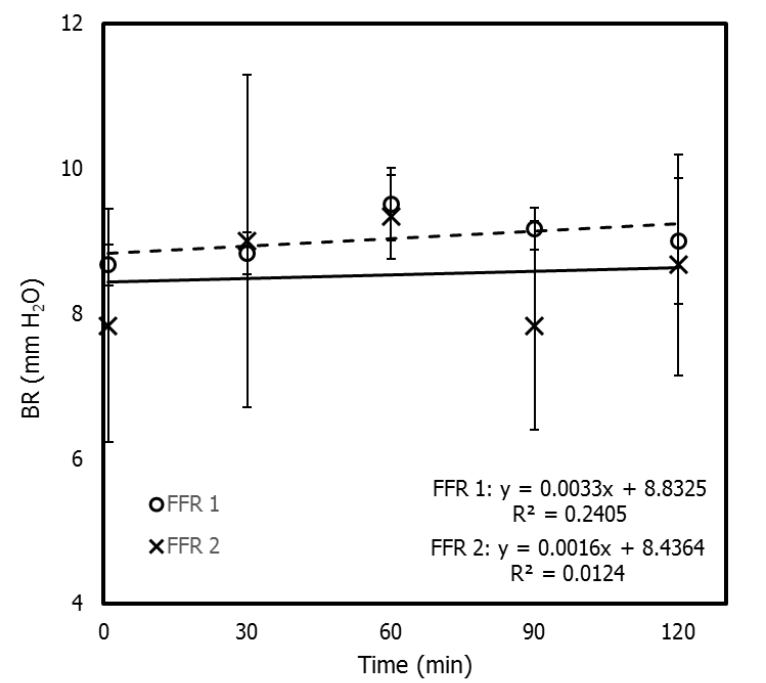

Figure 22. An example of the mean inhalation BR of FFRs measured during power washing

The slopes of the regression of the measured BR and the mean weight gain results of the FFRs grouped by rooms are shown in Table XI. Similar to the slopes of measured BR in Control Room, no increase was observed for FFR 1 in Test Room #1 ($p = 0.19$) and for FFR 2 in Test Room #2 ($p = 0.81$). No differences in weight gain were observed between FFRs when compared by Control Room ($p = 0.46$). Comparison of mass gained within FFRs and rooms showed significant differences between Test Room #1 and Control Room for FFR 2 (Table XI).

Table X. Breathing resistance slopes values (S_{BR}), mass gain (MG), temperature and relative humidity by swine rooms. (Mean ± S. D.)

FFR models	Control Room	Test Room #1	Test Room #2
FFR 1			
S_{BR} (mm H_2O min^{-1})	0.0033	0.0042	**0.0063**[1]
MG (g)	1.0 ± 0.1	1.3 ± 0.1	1.5 ± 0.3
Temperature (°C)	7.8 ± 1.5	15.4 ± 0.6	15.7 ± 1.7
Relative Humidity (%)	91.2 ± 9.6	90.2 ± 8.5	78.2 ± 9.9
FFR 2			
S_{BR} (mm H_2O min^{-1})	0.0016	**0.0084**[1]	-0.0004
MG (g)	1.1 ± 0.2	**1.8 ± 0.1**[2]	1.3 ± 0.4
Temperature (°C)	6.8 ± 1.2	18.0 ± 0.8	16.3 ± 1.3
Relative Humidity (%)	96.4 ± 6.0	88.6 ± 3.2	81.7 ± 8.1

[1] Bolded value is significantly different ($\alpha < 0.05$) from 0.
[2] Bolded value is significantly different ($\alpha < 0.05$) from the comparable Test Room value.

Discussion

In the present study, we have observed that BR of two FFRs did not increase while performing power washing in swine rooms for 120 min. Although this result differs from our result from a previous study where BR increased after testing two FFRs using simulated breathing and saturated air, 2, differences in airflow through the FFR and percent relative humidity levels may have an effect on BR. In Chapter 2 an airflow of 55 L min^{-1} was used to represent heavy breathing through the FFR and the air was kept at a relative humidity greater than 90% during the trial. In this study, the research member that performed the power washing did not experience heavy breathing while power washing. Based on worker experience during power washing, BR may not be a primary responsible for not using FFRs during the power washing task. Therefore, additional research is needed to determine other barriers for using FFRs while performing power washing tasks. Using FFRs during power washing is important for the prevention of adverse health effects among workers exposed to organic dust (Dosman et al. 2000; Zedja et al. 1993; Larson et al. 2002).

Power washing in this study was performed in small rooms in comparison to a typical commercial operations. This factor may have limited the time of power washing when compared to what may be found at large production swine farms. Power washing was conducted for each FFR for 120 min to compare BR under similar conditions. Larger swine production farms use a crew of workers to clean swine rooms. Therefore, the exposure observed during this study may not be representative of exposures experienced by workers during power washing on a large swine farm.

Changes in temperature and relative humidity during power washing were observed. These changes suggest, in general, that power washing decreases temperature but not enough to effect fan or heater activity. This observation is also corroborated by the measured relative humidity inside the room during power washing. Relative humidity remained above 90% and stable during power washing. Once power washing stopped, relative humidity decreased gradually until power washing started again. Some differences in temperature and relative humidity were observed between Test Rooms. However, as shown in Fig. 20 and Fig. 21, the entrance to Test Room #1 led to the outside, where temperature is uncontrollable, while the entrance to Test Room #2 led to an internal hallway where temperature was controlled by a heater.

A member of the research team performed all the power washing trials. Due to this fact, some conditions may be found that may have an impact on our results. First, the research member is not experienced in power washing swine rooms. Even though instructions were given on how to perform the power washing task by an experienced swine worker, other workers may perform power washing differently. Variability of FFR and UDM fit and breathing rate during the task was expected to be minimal as the same person performed the power washing.

There are several limitations in this study. An association between tested room and FFRs could not be established. Different results in BR of the tested FFRs used in Test Room #1 and Test Room #2 were observed. A combination of factors may arise during power washing that may impacted FFRs BR differently. Temperature, relative humidity, air movement inside the rooms, room size and configuration, winter season and time of power washing were recorded, additional factors not evaluated in this study may affects the FFR adversely. The present study focused on BR through two N95 FFRs models. Future study should be conducted to compare a larger number of FFRs models and increase the knowledge about FFRs performance. Also, particle penetration and faceseal leakage were not evaluated. FFRs with poor particle penetration and faceseal leakage during power washing may affect the feasibility of using FFRs as a protective device.

Conclusions

Breathing resistance of two N95 FFRs were evaluated while performing power washing in swine rooms. BR of the tested FFRs was unchanged during the 120 min trials. Therefore, workers using N95 FFRs while power washing may not have increased difficulty breathing with a new FFR, at least for the first 120 min of power washing. Based on this study, FFR wearer should expect no increase in BR over 8 hr of power washing, decrease health risk by wearing the FFR and no need to replace the FFR during the power washing task. A decrease in temperature and an increase in relative humidity was observed during the power washing task. The observed association suggests that temperature and relative humidity may create an uncomfortable environment during power washing in which the worker may think that it is more difficult to breathe through the FFR over the power washing time period. Further work is needed to substantiate this theory.

CHAPTER V

CONCLUSIONS

The work presented in this doctoral dissertation provide knowledge on assessing particle penetration and breathing resistance (BR) of filtering face-piece respirators (FFRs) and uncertified dust masks (UDMs). The first study investigated the effect of environmental conditions on the breathing resistance and particle penetration of two N95 FFRs. The second study determined the maximum particle penetration of UDMs. In addition, BR was evaluated against mass loading over time to compare BR between UDMs and FFRs. The third study evaluated N95 FFRs' breathing resistance while performing power washing in enclosed swine rooms.

Chapter II described the development of a sampling method to test particle penetration and BR of two FFRs under cyclic flow and different simulated air conditions. Sodium chloride (NaCl) Particle penetration was measured before and after the BR test using a scanning mobility particle sizer. BR was evaluated for 120 min against four different temperature and relative humidity conditions using a pressure transducer. Particle penetration through FFRs were found to be unaffected, retaining their particle capture capabilities. BR through the tested FFRs increased under high humidity conditions, however, the external layer of FFR 1 seemed to have moderated this effect.

Chapter III of this dissertation evaluated particle penetration of five different UDMs and the increase in BR of five UDMs and two FFRs against Arizona road dust (ARD). Particle penetration of UDMs were tested against NaCl and measured with a scanning mobility particle sizer. BR of UDMs and FFRs were tested against Arizona road dust in a one-direction airflow for 120 min. NaCl particle penetration through the tested UDMs were found to be between 3% to

75% at the most penetrating particle size. Increase in BR with mass loading were different for the UDMs and FFRs, even with testing the UDMs and FRRs against the same dust. It seems that different media style on the top layer of the UDMs and FFRs may affect the formation of the particulate dust cake and consequently, affecting BR through in tested models.

Chapter IV presented the field study of measuring BR of two N95 FFRs while performing power washing in swine rooms. Additionally, characterization of the environmental conditions generated during power washing were described. Power washing was performed on swine farms located in Iowa. A member of the research team wore the FFR while performing power washing inside the swine room. BR of the FFR was measured every 30 min for 120 min and after 120 min the worker switched the FFR. The findings of this study show that BR did not increased while power washing during the tested period. This study also showed that temperature and relative humidity varied by test rooms during the power washing task.

Future Work

Future studies are recommended to expand the evaluation of FFRs and UDMs presented in this dissertation. A limited number of FFRs and UDMs were evaluated. Additional FFRs and UDMs models should be tested to definitively confirm that our results are representative within other models. Testing other FFRs and UDMs models would also help identify different or similar physical properties that FFRs and UDMs have, may be leading to a design and development of new FFRs or UDMs.

Extensive laboratory test should be performed on the newly developed face mask. These tests may begin with assessing particle penetration and breathing resistance following NIOSH test protocol. Once NIOSH protocol has been approved, the face mask should then be tested for particle penetration and breathing resistance against other commercially available aerosols.

Finally, the face mask should be tested in filed studies get feedback form workers in accordance with the feasibility of wearing the face mask.

REFERENCES

Akbar-Khanzadeh, F. Bisesi, M. S. & Rivas, R. D. (1995). Comfort of personal protective equipment. *Applied Ergonomics*, 195-198.

Anthony, T. R., Altmaier, R., Park, J. H., Peters, T. M. (2014). *Modeled Effectiveness of Ventilation with Contaminant Control Devices on Indoor Air Quality in a Swine Farrowing Facility.* Journal of Occupational and Environmental Hygiene, 434-449.

Anthony, T. R., Altmaier, R., Jones, S., Gassman, R., Park, J. H., Peters, T. M. (2015). *Use of Recirculating Ventilation with Dust Filtration to Improve Wintertime Air Quality in a Swine Farrowing Room.* Journal of Occupational and Environmental Hygiene, DOI: 10.1080/15459624.2015.1029616

Balazy, A., Toivola, M., Reponen, T., Podgoeski, A., Zimmer, A., & Grinshup, S. (2006). Manikin-Based Performance Evaluation of N95 Filtering-Facepiece Respirators Challenged with Nanoparticles. *Ann. Occup. Hyg.*, 259-269.

Barrett, L., & Rousseau, A. (1998). Aerosol Loading Performance of Electret Filter Media. *American Industrial Hygiene Association Journal*, 538-539.

Belkin, N. (1996). A century after their introduction, aresurgical mask necessary? *Assoc. Oper Room Nurses J*, 602-607.

Bemer, D., & Calle, S. (2010). Evolution of the Efficiency and Pressure Drop of a Filter Media with Loading. *Aerosol Science and Technology*, 427-439.

BLS. (2002). *United State Department of Labor*. Retrieved July 30, 2015, from Bureau of Labor and Statistics: http://www.bls.gov/iif/home.htm

BLS. (2013). *United State Department of Labor*. Retrieved September 22, 2013, from Bureau of Labor and Statistics: http://www.bls.gov/oes/current/oes372011.htm

Brown, R. C. (1989). Modern Concepts of Air Filtration applied to Dust Respirators. *Ann. Occup. Hyg*, 615-644.

Cherrie, J., Howie, R., & Robertson, A. (1987). The Performance of Nuisance Dust respirators against typical Industrial Aerosols. *Ann. Occup. Hyg.*, 481-491.

Cho, H., & Yoon, C. (2012). Workplace Field Testing of the Pressure Drop of Particulate Respirators Using Welding Fumes. *Ann. Occup. Hyg.*, 948-958.

Cho, H.-W., Yoon, C.-S., Lee, J.-H., Lee, S.-J., Viner, A., & Johnson, E. (2011). Comparison of Pressure Drop and Filtration Efficiency of Particulate Respirators using Welding Fumes and Sodium Chloride. *Ann. Occup. Hyg.*, 666-680.

Cho, K., Reponen, T., McKay, R., Shukla, R., Haruta, H., & Sekar, P. (2010). Large Particle Penetration through N95 Respirators Filters and Faceseal Leaks with Cyclic Flow. *Ann. Occup. Hyg.*, 68-77.

Cho, K., Turkevich, L., Miller, M., McKay, R., Grinshpun, S., & Ha, K. (2013). Penetration of Fibers Versus Spherical Particles through Filter Media and Faceseal Leakage of N95 Filtering Facepiece Respirators with Cyclic Flow . *Journal of Occupational and Environmental Hygiene*, 109-115.

Contal, P., Simao, J., Thomas, D., Frising, T., Calle, S., Appert-Collin, J., & Bemer, D. (2004). Clogging of fibre filters by submicron droplets. Phenomena and influence of operating conditions. *Aerosol Science*, 263-278.

Doney, B. C., Groce, D. W., Campbell, D. L., Greskevitch, M. F., Hoffman, W. A., Middendorf, P. J., . . . Bong, K. M. (2005). A Survey of Private Sector Respirator Use in the United States: An Overview of Findings. *Journal of Occupational and Environmental Hygiene*, 267-276.

Donham, K. J., Reynolds, S. J., Whitten, P., Merchant, J. A., Burmeister, L., & Popendor, W. J. (1995). Respiratory Dysfunction in Swine Production Facility Workers: Dose-Response Relationships of Environmental Exposures and Pulmonary Function. *American Journal of Industrial Medicine*, 405-418.

Donham, K., Haglind, P., Peterson, Y., Rylander, R., & Belin, L. (1989). Environmental and health studies of farm workers in Swedish swine confinement buildings. *British Journal of Industrial Medicine*, 31-37.

Donham, K., Popendorf, W., Palmgren, U., & Larsson, L. (1986). Characterization of dusts collected from swine confinement buildings. *American Journal of Industrial Medicine*, 294-297.

Dosman, J. A., Senthilselvan, A., Kirychuk, S. P., Lemay, S., Barber, E. M., Willson, P., et al. (2000). Positive Human Health Effects of Wearing a Respirator in a Swine Barn. *Occupational and Environmental Lung Disease*, 852-860.

Durham, J., & Harrington, R. (1971). Influence of Relative Humidity on Filtration Resistance and Efficiency of Fabric Dust Filters. *Filtration and Separation*, 389-398.

Eshbaugh, J. P., Gardner, P. D., Richarson, A. W., & Hofrace, K. C. (2009). N95 and P100 Respirator Filter Efficiency Under High Constant and Cyclic Flow. *Journal of Occupational and Environmental Hygiene*, 52-61.

Fardi, B. a. (1991). Performance of disposable respirators. *Part. Part. Syst. Charact*, 308-3014.

Friedlander, S. (1958). Theory of Aerosol Filtration. *Aerosol Filtration*, 1161-1164.

Graveling R., Sanchez-Jimenez A., Lewis C. and Groat S. (2011) *Protecting Respiratory Health: What Should be the Constituents of an Effective RPE Programme?* Ann. Occup. Hyg, 230-238.

Grinshpun, S., Haruta, H., Eninger, R., Reponen, T., McKay, R., & Lee, S. (2009). Performance of an N95 Filtering Facepiece Particulate Respirator and a Surgical Masks during Human Breathing: Two Pathways for Particle Penetration. *Journal of Occupational and Environmental Hygiene*, 593-603.

Grupta, A., Novick, V., Biswas, P., & Monson, P. (1993). Effect of humidity and hygroscopicity on the mass loading capacity of high efficiency particulate air (HEPA) filter. *Aerosol Sci. Technol*, 94-107.

Gustafsson, B. (1997). The health and safety of workers in a confined animal system. Livestock Production Science, 191-202.

Guyton, H., Buchanan, L., & Lense, F. (1956). Evaluation of Respiratory Protection of Contagion Masks. *Appl Microbiol*, 141-143.

Hinds, W. (1999). *Aerosol Technology.* New York: Wiley Inter-science Publication.

Huang, S.-H., Chen, C.-W., Kuo, Y.-M., Lai, C.-Y., McKay, R., & Cheu, C.-C. (2013). Factors Affecting Filter Penetration and Quality Factor of Particulate Respirators. *Aerosol and Air Quality Research*, 162-171.

Janssen, L. (2004). Efficiency and Pressure Drop Effects of High concentrations of Cement dust on N95 Electret Filters. *Journal of the International Society for Respiratory Protection*, 75-82.

Johnson, A. (1993). How much work is expended for respirator? *Front. Med. Biol. Eng.*, 265-287.

Kongdee, A., Bechtold, T., Burtscher, E., & Scheinecker, M. (2004). The influence of wet/dry treatment on pore structure-the correlation of pore parameters, water retention and moisture regain values. *Carbohydrate Polymers*, 39-44.

Larsson, B.-M., Larsson, K., Malmberg, P., & Palmberg, L. (2002). Airways Inflamation After Exposure in a Swine Confinement Building During Cleaning Procedure. *Ammerican Journal of Industrial Medicine*, 250-258.

Larsson, K., Eklund, A., Hansson, L., Isaksson, B., & Malmberg, P. (1994). Swine Dust Causes Intense Airways Inflammation in Healthy Subjects. *Am J Respir Crit Care Med*, 973-977.

Letourneau, P., Mulcey, P., & Vendel, J. (1987). Effect of Dust Loading on the Pressure Drop and Efficiency of HEPA Filters. *Filtration & Separation*, 265-267.

Mardimae, A., Slessarev, M., Han, J., & et al. (2006). Modified N95 mask delivers high inspired oxygen concentration while effectively filtering aerosolized microparticles. Ann Emerg Med, 391-399.

Meyer, J. P., Hery, M., Herrault, J., Hubert, G., Francois, D., Hecht, G., & Villa, M. (1997). Field study of subjective assessment of negative pressure half-masks. Influence of the work conditions on comfort and efficiency. Applied Ergonomics, 331-338.

Miguel, A. (2003). Effect of air humidity on the evolution of permeability and performnce of a fibrous filter during loading with hygroscopic and non-hygroscopic particles. *Journal of Aerosol Science*, 783-799.

Mitchell D. C., & Schenker M. B. (2008). *Protection against breathing dust: behavior over time in Californian farmers*. Journal of Agricultural Safety and Health, 189-203.

Motyl, E., & Lowkis, B. (2006). *Effect of Air Humidity on Charge Decay and Lifetime of PP Electret Nonwovens*. Fibres & Textiles, 39-42.

NIOSH. (1995). *Respirator Protection Titlle 42, part 84.* Code of Federal Regulations.

NIOSH. (2005). *Determination of Exhalation Resistance Test, Air Purifying Respirators Standard Testing Procedure.* Pittsburgh.

Nonnenmann, M. W., Donham, K. J., Rautiainen, R. H., O'Shaughnessy, P. T., Burmeister, L. F., Reynolds, S. J. (2004). *Vegetable Oil Sprinkling as a Dust Reduction Method in Swine Confinement.* Journal of Agricultural Safety and Health, 7-15.

Novick, V., Higgins, P., Dierkschiede, B., Abrahamson, C., Richardson, W., Monson, P., & Ellison, P. (1990). *Efficiency and Mass Loading Characteristics of a typical HEPA Filter Media Material.* San Diego: Westinghouse Savannah River Report No. WSRC-RP90-779.

Novick, V., Monson, P., & Ellison, P. (1992). The Effect of Solid Particle Mass Loading on the Pressure Drop of HEPA Filters. *J. Aerosol Sci.*, 657-665.

OSHA. (2009). *Occupational Safety and Health Standards, Subpart I, Personal Protective Equipment, 1910.134, Respiratory Protection.* Washington: United States Department of Labor.

OSHA. (2014, 8 25). *United States department of Labor*. Retrieved 1 20, 2015, from www.OSHA.gov: https://www.osha.gov/SLTC/respiratoryprotection/index.html

O'Shaughnessy, P., Donham, K., Peters, T., Taylor, C., Altmaier, R., & Kelly, K. (2010). A Task-Specific Assessment of Swine Worker Exposure to Airbone Dust. *Journal of Occupational and Environmental Hygiene*, 7-13.

O'Shaughnessy, P., Peters, T., Donham, K., Taylor, C., Altmaier, R., & Kelly, K. (2012). Assessment of Swine Worker Exposures to Dust and Endotoxin during Hog Load-out and Power Washing. *The Annals of Occupational Hygiene*, 843-851.

O'Shaughnessy, P., & Raabe, O. (2003). A Comparison of Cascade Impactor Data Reduction Methods. *Aerosol Science and Technology*, 187-200.

Popendorf, W., Merchant, J., Leonard, S., Burmeister, L., & Olenchock, S. (1995). Respirator Protection and Acceptability Among Agricultural Workers. *Applied Occupational and Environmental Hygiene*, 595-605.

Rangasamy, S. (2011). Total Inward Leakage of Nanoparticles through Filtering Facepiece respirators. *Ann. Occup. Hyg.*, 253-263.

Rengasamy, S., BerryAnn, R., & Szalajda, J. (2013). Nanoparticle Filtration Performance of Filtering Facepiece Respirators and Canister/cartridge Filters. *Journal of Occupational and Environmental Hygiene*, 519-525.

Rengasamy, S., Eimer, B., & Shaffer, R. (2010). Simple Respiratory Protection—Evaluation of the Filtration Performance of Cloth Masks and Common Fabric Materials Against 20–1000 nm Size Particles. *Ann. Occup. Hyg.*, 789-798.

Roberge, R., Bayer, E., Powell, J., Coca, A., Roberge, M., & Benson, S. (2010). Effect of Exhaled Moisture on Breathing Resistance of N95 filtering Facepiece Respirators. *Ann. Occup. Hyg.*, 671-677.

Sharratt, B., & Auvermann, B. (2014). Dust Pollution from Agriculture. In N. Van Alfen, *Encyclopedia of Agriculture and Food Systems* (pp. 487-501). Esevier.

Shaviv, N. (2006, April). *Science Bits*. Retrieved March 13, 2013, from www.sciencebits.com: http://www.sciencebits.com/ExhaleCondCalc?calc=yes

Silverman , L., Lee, G., Flotkin, T., Sawyers, L., & Yancey, A. (1951). Air Flow Measurements on Human Subjects with and with-out Respiratory Resistance at Several Work Rates. *Industrial Hygiene and Occupational Medicine*, 461-478.

Siroka, B., Noisternig, M., Griesser, U. J., & Bechtold, T. (2008). Characterization of cellulosic fibers and fabrics by sorption/desorption. *Carbohydrate Research*, 2194-2199.

Stafford, R., Ettinger, H., & Rowland, T. (1973). Respirator Cartridge Filter Efficiency under Cyclic- and Steady-Flow Conditions. *American Industrial Hygiene Association Journal*.

Thomas, D., Penicot, P., Contal, P., Leclerc, D., & Vendel, J. (2001). Clogging of fibrous filters by solid aerosol particles experimental and modelling study. *Chemical Engineering Sciences*, 3549-3561.

US Department of Agriculture (USDA) (2014) 2012 Census of Agriculture: United States, Summary and State Data, Volume 1, Geographic Area Series Part 51 (AC-12-A-51).

Wang, Z., Larsson, K., Palmberg, L., Malmberg, P., Larsson, P., & Larsson, L. (1997). Inhalation of swine dust induces cytokine release in the upper and lower airways. *European Respiratory Journal*, 381-387.

Wake, D., & Brown, R. (1988). Measurements of the Filtration Efficiency of Nuisance Dust Respirators against Respirable and Non-Respirable Aerosol. *Ann. Occup. Hyg.*, 295-315.

Wake, D., Bowry, A., Crook, B., & Brown, R. (1997). Performance of respirator filters and surgical masks against bacterial aerosols. *J. Aerosol Sci.*, 1311-1329.

Zejda, J., Hurst, T., Barber, E., Rhodes, C., & Dosman, J. (1993). Respiratory Health Status in Swine Producers Using Respiratory Protective Devices. *American Journal of Industrial Medicine*, 743-750.